Aus der Klinik für Pädiatrie mit Schwerpunkt Neurologie
der Medizinischen Fakultät der Charité-Universitätsmedizin Berlin

DISSERTATION

„Development of a transgenic animal model for measurement of intra-cellular ATP“

zur Erlangung des akademischen Grades Doctor medicinae (Dr. med.)

vorgelegt der Medizinischen Fakultät Charité-Universitätsmedizin Berlin

von

Friederike Kristin Wilbert

aus Mainz

Datum der Promotion: 08.12.2017

Table of content

1 Zusammenfassung

Mitochondriopathien sind eine Gruppe klinisch heterogener, meist genetisch bedingter Multi-System-Erkrankungen, die auf einer eingeschränkten mitochondrialen Adenosintriphosphat (ATP)-Bereitstellung beruhen. Gewebe mit hohem Energiebedarf wie das Gehirn oder die Skelettmuskulatur sind vorrangig betroffen, Symptome wie epileptische Anfälle, Ataxie und Muskelschwäche sind häufig. Die zu Grunde liegenden Pathomechanismen sind bei weitem nicht vollständig verstanden. In diesem Kontext wäre die Messung kompartiment-spezifischer ATP-Spiegel ein interessanter Ansatz. Die vorliegende Dissertation behandelt die Fragestellung, ob die Erfassung und Quantifizierung des intramitochondrialen ATPs *in situ* mittels der Luciferase-Reaktion möglich ist. Dafür habe ich ein Genkonstrukt entworfen, welches aus dem Luciferase-Gen mit einer mitochondrialen Ziel-Sequenz besteht. Zusätzlich enthält das Konstrukt die kodierende Sequenz für das FLAG™-tag Peptid, welches den Nachweis des Konstruktes mittels eines spezifischen Antikörpers verbessert. Ausserdem fügte ich die Shine-Dalgarno-Sequenz, die für die optimale Translation in Prokaryoten erforderlich ist, und die Kozak-Sequenz, die das eukaryotische Startcodon beinhaltet, ein. Die Gensequenz wurde in das Plasmid pENTR1A_DS eingebracht. Dieser Vektor ist Teil des *Gateway® Recombination Systems*, einer Klonierungs-Methode, die sich des Mechanismus der ortsspezifischen Rekombination des Bakteriophagen *lambda* bedient. Dadurch ist die Klonierung des interessierenden Gens in verschiedene Vektor-Systeme deutlich einfacher. Ich erstellte sowohl einen Vektor zur Transfektion von Säugetier-Zellkulturen (pcDNA3.2/V5_cox8a-flag-luc), als auch einen Vektor zur Insertion des Konstruktes in den ROSA26-Locus muriner embryonaler Stammzellen (pROSA26_cox8a-flag-luc). Die Ergebnisse zeigen, dass die Transfektion von HEK293-Zellen mit pcDNA3.2/V5_cox8a-flag-luc zu einer Genexpression eines Proteins der Größe 70 kDa führt. Mittels Immunfluoreszenz konnte ich das Protein intra-mitochondrial lokalisieren. Die Funktionsfähigkeit des Proteins, welches als das Enzym Luciferase unter Anwesenheit von Luciferin und ATP Licht emittiert, konnte ich in transfizierten HEK293- und COS1-Zellen mittels des Luciferase-Assays nachweisen. Ein Luminometer erfasste die Licht-Emission in relativen Licht-Einheiten. Die Zufuhr steigender Mengen an Substrat (Luciferin) führte zu einer Erhöhung der Licht-Intensität. Ich entwickelte den zweiten Vektor, pROSA26_cox8a-flag-luc, für die Generierung eines *knock-in* Tiermodells mit konstitutiver, intra-mitochondrialer Luciferase-Expression. Das transgene Maus-Modell kann zum besseren Verständnis der Pathomechanismen von Mitochondriopathien beitragen.

2 Abstract

Mitochondriopathies are a group of clinically heterogeneous, mostly hereditary multisystemic disorders based on a deficient mitochondrial supply of ATP. Tissues with high energy demand, such as the brain or muscles, are predominantly affected. Symptoms include epileptic seizures, ataxia or muscle weakness. The underlying pathomechanisms are still not completely understood. In this context, the measurement of compartment-specific ATP levels represents an interesting approach. My doctoral thesis deals with the question whether the detection and quantification of intra-mitochondrial ATP *in situ* by means of the luciferase reaction would be possible. To explore this, I designed a gene construct containing the luciferase gene plus a mitochondrial targeting sequence and the antigenic fusion peptide FLAG™-tag. Additionally, I added the Shine-Dalgarno sequence, necessary for translation in prokaryotes, and the Kozak consensus sequence including the eukaryotic start codon. The gene sequence of interest was inserted into the plasmid pENTR1A_DS. This vector is part of the *Gateway® Recombination System*, a cloning tool based on the site-specific recombination pathway of the bacteriophage lambda being independent of appropriate restriction enzyme sites. This considerably facilitates cloning of fragments into different vector systems. I generated a vector for mammalian cell lines, (pcDNA3.2/V5_cox8a-flag-luc) and a targeting vector designed to insert the construct into the ROSA26 locus of the mouse (pROSA26_cox8a-flag-luc). I verified that transfection of HEK293 cells with the pcDNA3.2/V5_cox8a-flag-luc vector resulted in protein translation of a protein of about 70 kDa. By means of immunofluorescence, I identified the localization of the protein as intra-mitochondrial. I was able to confirm the functionality of the luciferase protein in transfected HEK293 and COS1 cells by means of a luciferin-luciferase assay. A luminometer detects the light emission in relative light units. Increasing amounts of the substrate luciferin led to a rise in light intensity. The second vector (pROSA26_cox8a-flag-luc) was constructed for the generation of a knock-in animal model with constitutive intra-mitochondrial luciferase expression. The transgenic mouse model will serve in future studies to bring forward the understanding of the pathomechanisms of mitochondriopathies.

3 List of abbreviations

ADP	adenosine-5’-diphosphate
ADP/O	adenosine-5’-diphosphate/oxygen
AgCl	silver chloride
AMP	adenosine-5’-monophosphate
APS	adenosine-5’-phosphosulfate
ATP	adenosine-5’-triphosphate
bp	base pair
BSA	bovine serum albumin
c	concentration
$CaCl_2$	calcium chloride
CO_2	carbon dioxide
CoA	coenzyme A
COX	cytochrome c oxidase
Cr	creatine
Cre	“causes recombination”
cyt c	cytochrome c
DAPI	4’,6-diamidino-2-phenylindole
ddH_2O	double-distilled water
ddNTPs	dideoxynucleotide triphosphates
DMEM	Dulbecco’s Modified Eagle Medium
DNA	deoxyribonucleic acid
DNP	2,4-dinitrophenol
dNTPs	deoxynucleotide triphosphates
DTT	dithiothreitol
ECL	enhanced chemiluminescence
EDTA	ethylenediamine tetraacetic acid
EGTA	ethylene glycol tetraacetic acid
ER	endoplasmatic reticulum
ES	embryonic stem
FAD	flavin adenine dinucleotide, oxidized form
$FADH_2$	flavin adenine dinucleotide, reduced form
FCCP	p-trifluoromethoxy carbonyl cyanide phenylhydrazone
Fig.	figure
FRET	fluorescence resonance energy transfer
G/M	glutamate/malate
GAPDH	glyceraldehyde 3-phosphate dehydrogenase
H^+	proton
H_2O	water
H_2O_2	hydrogen peroxide
HCl	hydrogen chloride
HPLC	high performance liquid chromatography
Hsp90	heat-shock protein-90
K_3PO_4	tripotassium phosphate
kbp	kilo base pair
KCl	potassium chloride
kDa	kilo Dalton
LB	lysogeny broth

M	mean
MELAS	Mitochondrial encephalomyopathy, lactic acidosis, and stroke-like episodes
MERRF	Myoclonic epilepsy with ragged red fibers
Mg^{2+}	magnesium
$MgCl_2$	magnesium chloride
min	minutes
MNGIE	myoneurogastrointestinal disorder and encephalopathy
mtDNA	mitochondrial DNA
N	amino
NaCl	sodium chloride
NAD^+	nicotinamide adenine dinucleotide, oxidized form
$NADH_2$	nicotinamide adenine dinucleotide, reduced form
Neo	neomycin
NMR	nuclear magnetic resonance
O_2	molecular oxygen, dioxygen
OXPHOS	oxidative phosphorylation
PAA	polyacrylamide
PBS	phosphate buffered saline
PCR	polymerase chain reaction
PCr	phosphocreatine
PET	positron emission tomography
PFA	paraformaldehyde
PGK	phosphoglycerate kinase
pH	negative logarithm of the hydronium ion activity
P_i	inorganic phosphate
pmf	proton motor force
P/O	Phosphate/Oxygen
polyA	polyadenylation
PP_i	pyrophosphate
Pt	platinum
Q	ubiquinone = coenzyme Q
RLU	Relative Light Units
ROS	reactive oxygen species
rRNA	ribosomal ribonucleic acid
SDS	sodium dodecyl sulfate
SDS-PAGE	Sodium Dodecyl Sulfate Poly-Acrylamide Gel Electrophoresis
SEM	standard error of the mean
S.O.C.	Super Optimal broth with Catabolite repression
SV40	Simian virus
TBE	Tris base, boric acid, EDTA containing buffer
TEMED	tetramethylethylenediamine
TMPD	tetramethyl-p-phenylenediamine
Tris	tris(hydroxymethyl)aminomethane
tRNA	transfer ribonucleic acid

4 Introduction

„Hold somebody's hand and feel its warmth. Gram per gram, it converts 10,000 times more energy per second than the sun. You find this hard to believe? Here are the numbers: an average human weighs 70 kilograms and consumes about 12,600 kilojoules/day; that makes about 2 millijoules/gram.second, or 2 milliwatts/gram. For the sun it's miserable 0.2 microjoules/ gram.second. Some bacteria, such as the soil bacterium "Azotobacter" convert as much as 10 joules/ gram.second, outperforming the sun by a factor of 50 million. I am warm because inside each of my body cells there are dozens, hundreds or even thousands of mitochondria that burn the food I eat."[1]

G Schatz in "Jeff's view on science and scientists".

4.1 Introduction to mitochondria

4.1.1 The morphology of mitochondria

The cell organelle we call "mitochondrion" today was first described in 1856 as filamentous (mito) and grain (chondrium)-like structures in muscle cells.[2] The shape of mitochondria varies from a small, spherical or "worm-like" shape to large clusters of mitochondria within one cell. Additionally, there is constant change between the different shapes. For this reason, the length of a mitochondrion varies between 10 μm and 50 μm (e.g. in the inner segments of the retinal photoreceptor cells). By means of electron-microscopy, the double membrane structure of the mitochondrion and the *cristae* were discovered.[3] The double membrane forms four different compartments of the mitochondrion: the plain outer membrane and the inner membrane that has many folds, the so-called *cristae*. The inter-membrane space lies between the two membranes, and inside the inner membrane we find the mitochondrial matrix. Mitochondria have a close spatial connection to the endoplasmic reticulum (ER) and the nucleus.[4,5,6,7] They are also very motile and can be transported along cytoskeletal tracks.[2]

4.1.2 The function of mitochondria

Mitochondria are called the "powerhouse of the cell".[8] Their main function is the allocation of energy in the form of adenosine-5'-triphosphate (ATP) for which they host three main biochemical energy-generating systems: the β-oxidation of fatty acids, the Krebs cycle, and the oxidative

phosphorylation (OXPHOS). The term **oxidative phosphorylation** refers to the coupling between the oxidation of nicotinamide adenine dinucleotide ($NADH_2$) and the phosphorylation of adenosine-5'-diphosphate (ADP) to ATP. A cell gains its energy through the processing of carbohydrates, fatty acids and proteins. During glycolysis, carbohydrates are metabolized anaerobically to pyruvate. Under aerobic conditions, pyruvate is transported into the mitochondrial matrix where it is coupled to coenzyme A (CoA) and introduced into the Krebs cycle. Fatty acids are imported into the mitochondrial matrix through several intermediate steps involving carrier molecules (e.g. carnitine). After β-oxidation in the mitochondrial matrix, they are also introduced as acetyl-CoA compounds into the Krebs cycle. Amongst others, the Krebs cycle generates $NADH_2$ and flavin adenine dinucleotide ($FADH_2$), thus providing the respiratory chain with its substrates. There is an ongoing discussion about the exact number of ATP molecules generated per oxidation of $NADH_2$/ $FADH_2$: 1 $NADH_2$ > ≈2.5 ATP, 1 $FADH_2$ > ≈1.5 ATP, one passage of the Krebs cycle > ≈10 molecules of ATP.

The **respiratory chain** is a system of enzyme complexes, which serve as electron acceptors and donors (see Figure 1). It contains five large complexes (I-V) located at the inner mitochondrial membrane: the NADH:ubiquinone oxidoreductase (Complex I), the succinate dehydrogenase (Complex II), the ubiquinol:cytochrome c oxidoreductase (Complex III), the cytochrome c oxidase (Complex IV, COX) and finally the F_1F_o-ATP synthase (Complex V). The electrons pass through the complexes in a determined order until they are transferred onto molecular oxygen (O_2). The passage of electrons releases energy that is used to pump protons from the mitochondrial matrix into the inter-membrane space. The trans-membrane potential of ≈150-180 mV (depending on the pH value) established in this manner drives the ATP synthase and leads to the conversion of ADP and inorganic phosphate (P_i) to ATP.[9] This theory was first formulated as the "chemi-osmotic hypothesis" by the later Nobel laureate Mitchell in 1961.[10] The ATP/ADP transporters at the inner membrane and the voltage-dependent anion channels at the outer membrane export ATP into the cytoplasm. Here, the ATP can be used for further processes within the cell. This explains why the number of mitochondria in a cell depends on the need for energy for specific cell functions. It can therefore also change in the course of a cell's lifetime. In order to investigate the integrity of the respiratory chain, researchers can block the different complexes separately by adding specific inhibitors (see Figure 2). Those substances are amongst the most potent cell poisons. Taken together, they all lower the ATP production and oxygen consumption.

Additionally, there is the possibility of uncoupling of the respiratory chain. An uncoupler short-circuits the protons from the inter-membrane space into the mitochondrial matrix. It thereby destroys the proton membrane gradient and deprives the ATP synthase of its driving power. A

physiological uncoupling protein is thermogenin, synthetic substances are dinitrophenol (2,4-dinitrophenol, DNP) or FCCP (p-trifluoromethoxy carbonyl cyanide phenylhydrazone).

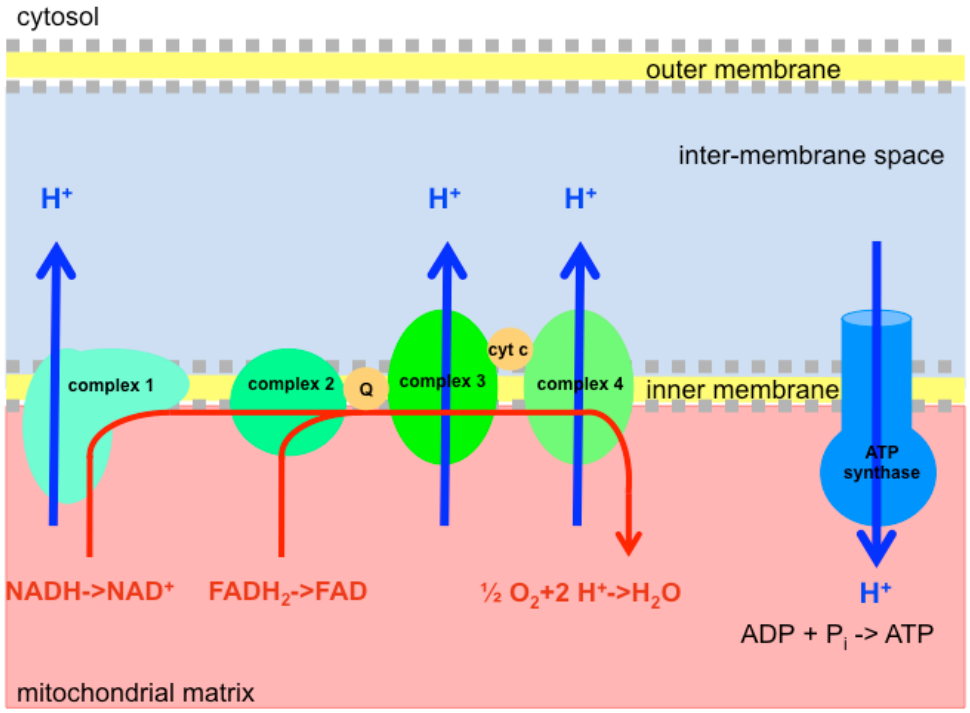

Figure 1: The respiratory chain. Electrons of NADH and $FADH_2$ are transported by means of the soluble molecules ubiquinone and cytochrome c and are transferred to molecular oxygen. Protons flow into the inter-membrane space. The reflux of protons through the ATP synthase generates energy used for the synthesis of ATP.

enzyme	**inhibitor**	**function of inhibitor and consequences**
Complex I	rotenone	blocks the ubiquinone binding site; oxidative phosphorylation is still possible
	amobarbital	
Complex II	malonate	competitive inhibitor of the succinate dehydrogenase; leads to accumulation of succinate[11]
Complex III	antimycin A	blocks complex III between cytochrome b and cytochrome c_1; oxidation of NADH and succinate is not possible[12,13]
	myxothiazol	leads to complete oxidation of cytochrome c, c_1 and cytochrome oxidase, while the b cytochromes remain reduced[14,15]
Complex IV	cyanide	blocks the binding site of O_2; no more reduction of O_2, respiratory chain stops
	azide	
ATP synthase	oligomycin	binds to the F_o-subunit, stops its rotor movement, accumulation of protons in the inter-membrane space, hyperpolarization of membrane potential, no flux of protons into the inter-membrane space, respiratory chain stops

Figure 2: Inhibitors of the enzymes of the OXPHOS system.

Other functions that are located in the mitochondrion are the urea cycle, the regulation of programmed cell death (apoptosis), the production of reactive oxygen species (ROS = free peroxide, oxygen and superoxide radicals), and the buffering of calcium.

4.1.3 Mitochondrial genetics

A unique feature of the mitochondria among all cell organelles of the animal cell is their own genome. It is a circular double-stranded deoxyribonucleic acid (DNA) molecule of 16,569 base pairs.[16] It encodes 13 subunits of the respiratory chain complexes (Complex I, III, IV and V), 22 mitochondrial transfer ribonucleic acids (tRNA) and two mitochondrial ribosomal nucleic acids (rRNA). The replication of the mitochondrial DNA (mtDNA) takes place separately from the nuclear DNA. Mitochondria multiply by fission, a process that is independent of the eukaryotic cell cycle. The **endosymbiotic theory** gives a possible explanation for the relative "independence" of the mitochondria within a cell.[17] Lynn Margulis postulated in the seventies that mitochondria evolved from aerobic proteobacteria, which were able to perform oxidative phosphorylation. The aerobic proteobacteria lived in symbiosis with the eucaryotic precursor cells, which could only perform glycolysis and had to eliminate lactate or pyruvate. In a second step, the proto-proteobacteria were incorporated into the primitive eukaryotic cells by engulfment into the membrane of the host. This process might explain the double membrane of a mitochondrion, its circular DNA, and the absence of a nucleus and of histones. In the course of evolution, the reciprocal dependency increased and parts of the mitochondrial genome were integrated into the nuclear genome of the host. The transcription of these nuclear encoded proteins of the mitochondria takes place in the nucleus and their translation in the cytosol at the endoplasmic reticulum. After processing in the Golgi apparatus, they are transported into the mitochondria and sorted to their sub-mitochondrial target compartments by means of specific N-terminal mitochondrial signaling peptide sequences.

There are further peculiarities of mitochondrial genetics:

[1] The mitochondrial genome has a higher **susceptibility to mutations** than the nuclear genome.[18] The mutation rate of the mitochondrial genome is up to ten times that of the nuclear DNA.[19] One of the reasons is that, in contrast to nuclear DNA, the mtDNA is exposed to higher concentrations of ROS generated by the oxidative phosphorylation. As mtDNA lacks histones, it is less protected in general. Moreover, the repair mechanisms of the mtDNA are not as efficient as those of the nuclear DNA. Finally, the density of encoding genes is higher in the mtDNA due to the absence of introns in animal mitochondria leading to an increased susceptibility to mutations.

[2] A somatic cell has about 100 to 1,000 mitochondria, each of which contains two to ten **mtDNA copies**. The average mtDNA copy number of a somatic cell is about 10^3 to 10^4.[20] The overall amount differs in somatic cells of different tissues according to their energy demand.[21]

[3] Heteroplasmy is the permanent presence of two, sometimes of even more, mitochondrial genotypes in a cell, an organ or an individual. One type is considered "wild-type", whereas the other carries a mutation or a variant. The mutation is either a spontaneous somatic mutation or has been transmitted through the maternal germ line (see above). The level of heteroplasmy is indicated by the percentage of affected mtDNA copies (of all mtDNA copies) of a cell or tissue and shows a large variability between different cells, tissues and individuals.[22]

[4] The inheritance of mammalian mitochondrial DNA does not follow the Laws of Mendel, but is only passed on through the oocyte (**maternal inheritance**).[23] The underlying mechanisms are not only the huge difference in mtDNA copy numbers between a sperm and an ovum, but also the impossibility of paternal mitochondria to cross the cell envelope of the ovum[24] or even the active removal of paternal mitochondria from the plasma of the oocyte.[25,26] Only one case of paternal inheritance was reported.[27]

[5] During mammalian oogenesis in a female embryo, mitochondria are selected through a radical reduction of the number of mitochondria per precursor cell (*bottleneck hypothesis*).[28] In subsequent cell divisions, the mitochondria are distributed arbitrarily to the daughter cells by **mitotic segregation**. Consequently, each of these daughter cells can possess healthy/unaffected/wild-type or mutated/affected mitochondria. The number of mutated mtDNA copies needs to reach a certain mutation-specific threshold before a clinical phenotype will be seen in a patient.[29]

4.1.4 Mitochondriopathies

The prevalence of mitochondriopathies is estimated to lie between 1:10,000 and 1.31:10,000 in children.[30,31] Mitochondriopathies are the most prevalent metabolic inherited diseases, with an incidence of about 1:5000 live births.[32] They are a clinically heterogeneous group of diseases caused by genetic defects of the entire metabolic pathway of pyruvate oxidation. It comprises dysfunctions in the pyruvate dehydrogenase complex, the Krebs cycle, or the oxidative phosphorylation as well as the relevant mitochondrial membrane transport systems.[33] Additionally, mtDNA replication, maintenance and processing or mtRNA translational machinery may be damaged.[34] The causative genetic alteration can be found either in the mitochondrial genome or in the nuclear genome that encodes most of the mitochondrial proteins.[35] The mutation(s) may affect structural proteins or assembly factors of the subunits of the enzyme complexes. Proteins that regulate mitochondrial metabolism and their interaction with the nucleus may be equally

affected. As mitochondria are ubiquitous, every organ can be harmed by mitochondrial dysfunction, with tissues with elevated energy requirements (e.g. the brain and the muscle) being most frequently affected. The resulting clinical phenotypes are very variable. The same mutation in two individuals can result in completely different phenotypes (=genetic variability), whereas different mutations may induce very similar symptoms (=genetic heterogeneity). Furthermore, the age of manifestation ranges from the neonatal period to adulthood.[36] Similarly, the clinical course can vary from a faintly discernible disorder to severe disease and death. Because of this variability, it is difficult to establish a classification of mitochondriopathies based on the clinical phenotype alone. To the author's knowledge, there is no uniform international classification to date. However, there are some attempts to classify the heterogeneous pool of several hundred different mitochondrial disorders into subgroups.[37] One is the differentiation between "mitochondrial syndromes", "mitochondrial encephalomyopathies" and "mitochondriopathies with primarily non-neuropathic symptoms", as proposed by the German guideline for mitochondriopathies in children and adolescents.[33] The first group comprises the classic mitochondrial disorders that are defined by a combination of specific symptoms. Examples are the syndromes "mitochondrial encephalomyopathy, lactic acidosis, and stroke-like episodes" (MELAS) and "myoclonic epilepsy with ragged-red-fibers" (MERRF). The most common mitochondrial diseases in children are encephalomyopathies; affected patients often suffer from epilepsy as well as heart/skeletal muscle weakness. Finally, the third category accommodates the fact that mitochondria are ubiquitous, and comprises disorders in which the neurological impairment is not prominent. This criterion applies to diseases such as a "myo-neuro-gastro-intestinal disorder and encephalopathy" (MNGIE), caused by thymidine phosphorylase deficiency, and malignancies attributed to the down-regulation of Complex II activity (e.g. gastro-intestinal stroma tumors, pheochromocytoma).

Discovering the molecular basis of mitochondrial disorders is challenging and time-consuming. The gold standard of clinical diagnostics is considered to be the biochemical analysis of the respiratory chain function in most severely affected tissues. As brain tissue is not accessible in most cases, these investigations are mainly done on muscle biopsy specimens or on cultured human fibroblasts. The diagnostic studies are completed by a molecular analysis of candidate genes, based on the identified biochemical defect. In the case of characteristic mitochondrial syndromes, such as MELAS or MERRF, the biochemical analysis can be bypassed and the diagnostic studies should start with a search for the pathogenic mutation in the mtDNA.[38]

4.1.5 Measurement of ATP levels and ATP production

Genetic defects in mitochondriopathies often cause a net reduction of ATP synthesis. It has been proved in human skin fibroblast cultures with disease-causing mutations that ATP content was lower.[39,40] Many different genetic or exogenic factors may be responsible for such a scenario. For this reason, the existence of a molecular tool to quantify ATP content and turnover in living tissues and organisms would be desirable, as it is *the* common denominator of mitochondrial disease.

In striving to establish such a method, one has to consider that an eukaryotic cell has two main pathways for ATP generation from fuel molecules (sugars, fats, proteins).[41] The first is **glycolysis,** taking place in the cytosol, and the second is **oxidative phosphorylation**, depending on the specialized double membrane system of the mitochondrion. The latter is much more efficient: 1 mol glucose produces 2 mol ATP *via* glycolysis in the cytosol and an additional 36 mol ATP *via* oxidative phosphorylation. Therefore, it would be crucial to differentiate between ATP generated in the cytosol and that generated in the mitochondria.

The most obvious method would be the measurement of the metabolite ATP itself. Other options are the measurement of membrane potentials or the analysis of the mitochondrial proton current (see chapter 4.1.6). Currently, the most widely used tool to detect and measure ATP is firefly luciferase.[42] The enzyme converts its substrate luciferin to oxyluciferin, thereby emitting light and consuming ATP as a co-substrate. The light intensity depends on the available ATP. The emitted light can be quantified by means of luminometry (see chapter 4.2).[42]

4.1.6 *In vitro* measurement of ATP

It is possible to investigate cellular ATP content *in vitro* or *in vivo*. "*In vitro*" means the analysis of parts of an organism that are separated from their original biological context. Essential examples are isolated mitochondria, permeabilized cells and intact cells taken from a cell culture. "*In vivo*" describes experiments that are carried out in living organisms as for example in moving animals.

While performing *in vitro* kinetic assays, there are two elements of mitochondrial bioenergetics that depend on the proton flow through the inner mitochondrial membrane.[43] These are the **membrane potential** or **proton motor force** (pmf, in mV) and the **flux** or **proton current** (in nmol of protons/min). The pmf comprises two measurable values: first, the pH difference between the mitochondrial matrix and the inter-membrane space, which depends on the number of protons present in the inter-membrane space. The second is the mitochondrial membrane potential, which is defined as the voltage-gradient between the cytoplasm and the mitochondrial ma-

trix. The flux is determined by the amount of protons that pass the inner mitochondrial membrane.

With regard to the measurement of ATP, two conditions need to be distinguished. When ATP is synthesized, the ATP synthase represents the main pathway of proton re-entry into the mitochondrial matrix. Under these circumstances, the pmf is lowered and consequently the respiratory chain increases its electron flux. If the ATP turnover is determined, the mitochondrial respiration should be gradually reduced by titration of respiratory chain inhibitors. If no ATP is synthesized (e.g. in the "decoupled state"), all protons re-enter the matrix through a proton leak, which is caused by uncoupling proteins or by organic compounds (e.g. FCCP). Beyond these "artificial" states, all mitochondria have a naturally occurring endogenous proton leak. Brand & Nicholls stress the point that the endogenous proton leak is inherent to all mitochondria and is not a problem caused by isolation of mitochondria.[43] For the final interpretation of results, the relevant endogenous proton leak needs to be considered.

Isolated mitochondria have been exhaustively studied and corresponding techniques are well established. Mitochondria can be extracted from many tissues of wild-type or mutated organisms. The cells need to be lysed by various methods if the experiment is carried out with isolated mitochondria: Permeabilization and rupture of cells can be performed by using detergents such as digitonine or Triton X-100 with subsequent pottering and differential centrifugation in sucrose gradients. Investigation of isolated mitochondria is the preferred method for studies of mitochondrial bioenergetics. Even hydrophilic substrates rapidly gain access to the mitochondrial membranes. An assay of isolated mitochondria is usually normalized either to the mitochondrial mass or the mtDNA or cytochrome C content.[44] However, isolated mitochondria are very fragile, and a large number of mitochondria are needed for each assay. They can be damaged during the process of isolation, which depends on the kind of tissue/cells (e.g. isolated cells from culture *versus* whole organs such as muscles).

Investigations of permeabilized cells are comparable to those of isolated mitochondria. While working with permeabilized cells, the steps of cell lysis and preparation of mitochondria are skipped. Hence, one does not encounter the associated problems such as impairment or loss of mitochondria. Furthermore, the use of permeabilized cells is time saving. Another advantage is the maintenance of the integrity of other cell organelles. However, one should take into account a lower purity of mitochondria and the presence of interfering factors from other cell components and organelles. The permeabilization reagent may damage the outer mitochondrial membrane, leading to cytochrome C release and apoptosis.

In intact cells, ATP production is integrated into its physiological environment. Cell lines can be manipulated genetically and are available for plate-based assays. However, the experimental system is more complex, the interpretation of results can be difficult. Additionally, the cell membrane is not permeable to many reagents and methods are not quantitative enough. Lastly, the cell-based system still does not represent the context of a whole organ or even organism.[43]

4.1.7 Dynamic measurement of ATP

On one hand, the ATP production rate, and, more specifically, the phosphorylation rate of ADP to ATP, is responsive to altered ATP demand in the cell. On the other hand, the increase in ATP production depends on the functional integrity of the four respiratory chain complexes and of the ATP synthase. Hence, inhibition of any of these enzymes has an impact on the ATP synthesis. The integrity of the respiratory chain complexes can be determined by measuring the oxygen consumption of a cell. A proton gradient is generated and electrons are transferred to molecular oxygen only if these enzymes work properly. In order to analyze the oxygen turnover, one has to employ experimental techniques that are based on **polarography**, e.g. the measurement of oxygen consumption using a Clark-type oxygen electrode (Figure 3).[45] In order to measure the maximum flux through the respiratory chain, the oxygen consumption and the ATP production are decoupled, e.g. by the use of DNP. However, this experiment cannot be used to determine the production of ATP, the final "goal" of the respiratory chain, in a dynamic setting.

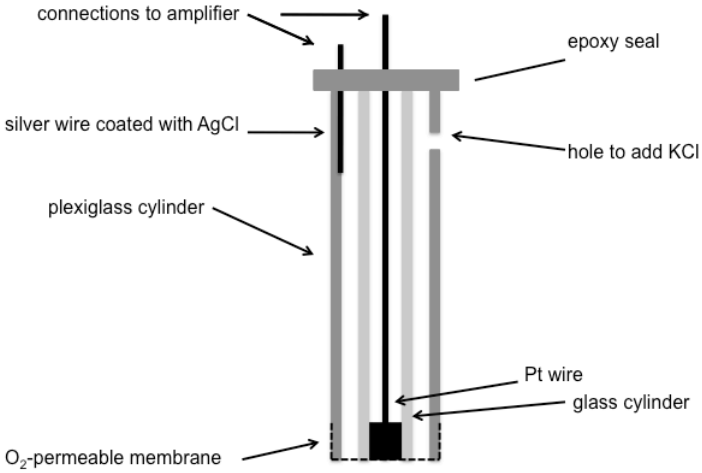

Figure 3: Clark-type oxygen electrode. AgCl=silver chloride, KCl=potassium chloride, Pt wire=platinum wire.

The measurement of the Phosphate/Oxygen (P/O) ratio in permeabilized cells determines ATP production indirectly. The P/O ratio indicates the coupling of the mitochondrial respiration to ATP production and serves as a parameter for the efficiency of oxidative phosphorylation.[46] The P/O ratio is defined as "moles of ATP produced per moles of oxygen consumed during ADP-stimulated […] respiration".[46] The P/O ratio is determined by means of an oxygraphic chamber that measures the oxygen content within a hermetically closed space or volume of fluid. The amount of the added substrate ADP is considered, too. Chance and Williams showed that one can equate the P/O ratio with the ADP/O ratio, since almost all externally added ADP is utilized in oxidative phosphorylation.[47]

4.1.8 Measurement of ATP steady-state levels

The term "steady-state" describes a condition, in which the outward proton current and the inward proton current across the inner mitochondrial membrane are balanced.[43] In 1955, Chance & Williams established a series of oxygen electrode experiments in order to examine the mitochondrial function. They named a distinct step of their experiment a "state" that is defined by the substrate added and the consequent behavior of the electron transport, proton motor force, proton transport and respiration.[47] Chance & Williams distinguished six different "states" (Figure 4):[48]

state	characterization
"state 1"	Addition of isolated mitochondria to an oxygraphic chamber containing a solution supplied with oxygen and inorganic phosphate, but no ADP. No ATP synthesis. Leak respiration due to endogenous substrates that are slowly consumed.
"state 2"	Addition of ADP, but limited substrate. Intermittent increase of oxygen flux by ADP and oxidation of residual endogenous substrate. Steady "state 2": low oxygen flux, high ADP level.
"state 3"	High ADP and P_i concentrations, defined reduced substrate or substrate combination, sufficient oxygen concentration. In order to measure the OXPHOS capacity, ADP and P_i concentrations need to be saturated. Respiration is partly coupled and either partly uncoupled (physiological) or partly "dyscoupled" (pathological).
"state 3u"	Uncoupled state, the respiratory chain complexes are completely uncoupled from the ATP synthase. "State 3u" is artificially induced in order to determine the electron transfer system capacity of the respiratory chain.
"state 4"	"state 4" follows necessarily "state 3","state 4" is characterized by a depletion of ADP. ADP is completely converted into ATP, caused by the electron transfer from defined reduced substrates to oxygen. Phosphorylation is not possible, except the case if ATPase provides recycled ADP
"state 4o"	Inhibition of the ATP synthase with oligomycin, in order to control whether ADP is provided by ATPase.
"state 5"	Final phase after the passage from "state 1" to "state 4", oxygen in the closed oxygraphic chamber is completely consumed, anaerobic state.

Figure 4: States of mitochondrial respiration as defined by Chance & Williams (1955).

4.1.9 Discrimination between cytosolic and mitochondrial production of ATP

For the measurement of ATP levels, one has to differentiate between cytosolic or mitochondrial ATP. One reason is that the total amount of cytosolic ATP does not only depend on the mitochondrial function, but is also influenced by the metabolism of adenine nucleotides in the cytoplasm (e.g. lipolysis or glycolysis) and the efflux of ATP from the mitochondria. A change of the cytosolic ATP concentration cannot clearly be attributed to the one or the other source.[43]

4.1.10 *In vivo* measurement of ATP

Two main methods of *in vivo* measurement are known: first, the **luciferin-luciferase system** and second the imaging techniques based on nuclear magnetic resonance (NMR) as for example NMR-spectroscopy. The first method is applicable to organisms that are genetically modified *via* insertion of the luciferase gene but offers cellular resolution. The latter method can be applied to whole organisms, but it requires expensive equipment (MR spectrograph) and has a lower spatial resolution. In my work I concentrated on the Luciferin-luciferase system.

4.2 The luciferin-luciferase system

The current, most commonly used method to measure intra-cellular ATP utilizes **firefly luciferase**.[42] This system can be applied to isolated mitochondria and to intact cells. It allows measuring ATP within different organelles of living cells by measuring the resulting light signal from bioluminescence. Measurements can be performed at single time points or continuously.

4.2.1 Bioluminescence

The luciferin-luciferase system is based on the phenomenon of **bioluminescence**. The term bioluminescence derives from the Greek word βίος, "living", and the Latin word *lumen*, "light". According to Greer, "bioluminescence is a chemiluminescent reaction between at least two molecules produced under physiological conditions within or in association with an organism."[49] In other words, bioluminescent proteins turn chemical bond energy into light energy.[50] A chemical compound becomes excited by the free energy of a chemical reaction (e.g. an oxidation) and the emission of photons is the result of the relaxation of this excited compound to its energetic base level.[50] The presence of oxygen and of intermediary peroxides is needed in every type of known bioluminescence reaction.[51]

4.2.2 The components of the luciferin-luciferase system

Firefly luciferase is a 63 kilo Dalton (kDa) protein that catalyzes the production of light (Protein Data Bank accession number 1LCI). It originates from the North American firefly *Photinus pyralis*.[52] In the presence of molecular oxygen, it oxidizes its substrate luciferin in a light-producing reaction, in which ATP is a mandatory co-substrate and a magnesium ion a cofactor (Figure 5).[53] The reaction consists of two steps:

1. Reaction of luciferin with ATP and a metallic cation to inorganic pyrophosphate and the intermediate luciferyl-adenylate,
2. Oxidation and decarboxylation of luciferyl-adenylate to oxyluciferin, which is the light-emitting reaction.

The oxidation of firefly luciferin is the most efficient bioluminescent reaction known to date. It has a high quantum yield of 0.88 of luciferin.[54] In this context, quantum yield is a measure for "[…] the fraction of molecules that emit a photon after direct excitation […]".[55] The wave length of light emission characteristically lies between 550 and 570 nm (yellow-green region) with a peak at 562 nm at neutral pH (approximately 7.5-7.8) (see Figure 5).[56] A shift of the emission spectrum can be observed if firefly luciferase is exposed either to an alteration of pH, a change of temperature or the addition of a metal cation.[56]

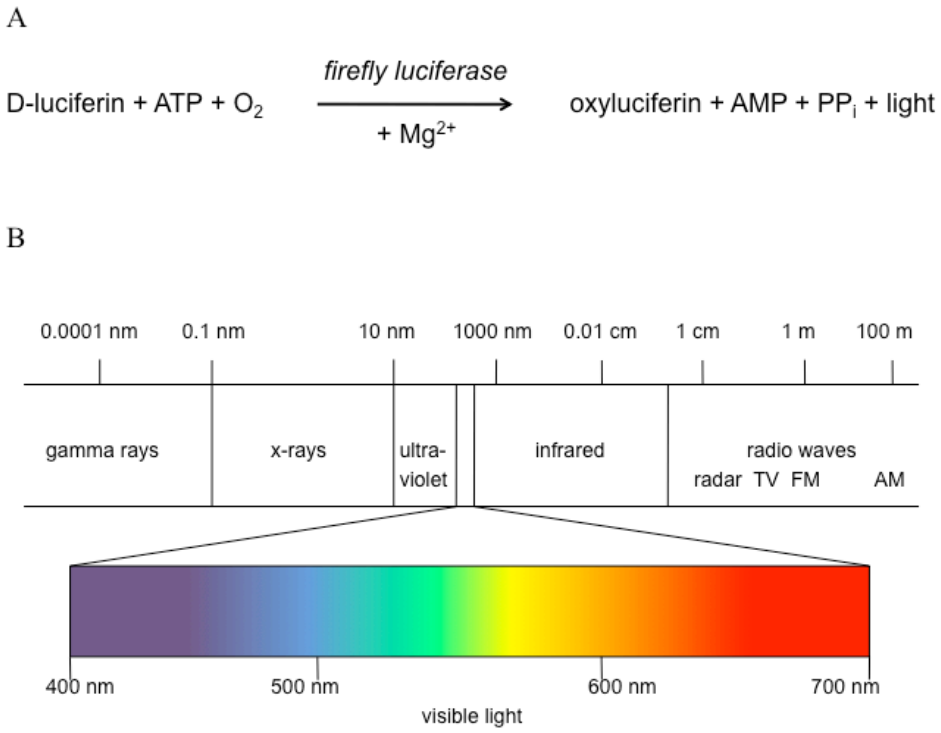

Figure 5: (A) Reaction catalyzed by firefly luciferase. (B) Spectrum of light. Luciferase emits green-yellow light between 550 and 570 nm.

Since luciferase was primarily found in firefly species, the first experiments were performed by grounding living fireflies. In the following years, protocols based on the processing of only the lanterns of firefly species were developed.[53] In 1985, DeWet and his coworkers succeeded in cloning the luciferase gene, which enabled the recombinant expression of active firefly luciferase in *E. coli*.[57] A little later, they reported the successful expression of luciferase in mammalian cells.[58] Neufeld showed that the resulting light emission was a linear reproducible response to the luciferase concentration applied.[59] Another influencing factor is the concentration of the substrate luciferin.[60] **Luciferin** is the luminescence molecule that is commonly used as substrate in luciferase catalyzed reactions.[53,57] Its structure was identified as benzothiazole.[61] Firefly luciferase is stereospecific: D-luciferin as well as L-luciferin react with ATP to pyrophosphate. However, only the D-luciferin isomer contributes to light production.[62] **Coenzyme A** (CoA) increases the light intensity by up to two-fold and extends the duration of light emission. This is due to the better reaction kinetics of luciferase with luciferyl-CoA. Coenzyme A removes the inhibiting oxyluciferin from the binding site of luciferase.[63,64]

The need of **ATP** for light emission was first described by McElroy in 1947.[65] He grounded living fireflies and observed luminescence that diminished rapidly. McElroy mentioned that the duration of light emission depended on the amount of ATP. He compared the results after the addition of ATP at low concentrations to those achieved by high concentrations. The latter yielded a longer lasting light emission. He showed that the light intensity was proportional to the ATP concentration. ATP was found to be an allosteric modulator of luciferase.[66] Due to its specificity for ATP, firefly luciferase is often employed to quantify ATP in biological samples.[67] To measure intracellular ATP, cells have to be lysed and enzyme (luciferase) and substrate (luciferin) added.[59] The molecule ATP is also synthesized by pathways other than the oxidative phosphorylation, therefore, the origin of ATP and thus the source of luminescence need to be determined. The inhibition of one of the ATP-generating pathways would be helpful. P^1,P^5-di(adenosine) pentaphosphate inhibits the cytosolic adenylate kinase. In reverse, the assessment of the luminescence that does not derive from mitochondrial ATP could be determined using inhibitors of mitochondrial ATP synthesis such as oligomycin.[44]

Luciferase assays are widely used as **reporter gene** systems.[63,67,68] A reporter gene encodes an easily detectable product. The reporter gene is attached to a promoter of interest and thus enables quantification of gene expression from specific promoters. Kennedy *et al.* and Jouaville *et al.* suggested the possibility of measuring ATP levels by means of targeted luciferase.[60,69] Its use allows measuring ATP production inside different organelles of living cells by measuring the resulting light signal.

In order to target the luciferase into the mitochondrial matrix, a targeting sequence is needed. Most of the proteins found in mitochondria are encoded by nuclear DNA and translated at the endoplasmic reticulum. These proteins have a signal peptide that is responsible for the correct subcellular positioning. Rizzuto *et al.* investigated this mitochondrial-targeting system and found that the amino(N)-terminal 33 amino acids of the subunit VIII of cytochrome c oxidase protein (*Cox8*) constitute an efficient targeting sequence.[70,71] It comprises a pre-sequence of 25 N-terminal amino acids that are partially cleaved after mitochondrial import to generate the mature polypeptide. Successful positioning of the targeted protein can be verified by immunocytochemistry with an anti-luciferase antibody.

4.3 The aim of the study

Researchers assume that the clinical symptoms of mitochondriopathies are mainly caused by a lack of ATP. The possibility to measure ATP levels *in vivo* in different organs of a living animal would be a crucial step in the understanding of the variability of mitochondrial disorders. The generation of such a mouse model was planned by the research group of Professor Schülke at the Department of Neuropediatrics, Charité, Berlin. The aim of my work was the preparation, assembly, cloning and testing of a gene construct that would result in an intra-mitochondrially located luciferase enzyme in order to detect the mitochondrial ATP content.

I chose the well-established luciferin-luciferase system as a tool for the analysis of ATP. I created two vectors, the first for expression in cultured mammalian cells after transfection, the second for the generation of a transgenic mouse model. In this process, the *luc* gene sequence had to be complemented with sequences allowing eukaryotic and prokaryotic translation, protein import into the mitochondrial matrix and detection by an antibody. The cloning was facilitated by the use of the *Gateway® Recombination System* in addition to standard molecular biological methods. The first vector should be used to verify the protein size, localization and function *via* expression in a mammalian cell culture system. If these tests would be successful, a transgenic knock-in mouse was to be developed *via* homologous recombination of the construct into the ROSA26 locus of murine ES cells and subsequent blastocyst injection of positive ES clones. Activation of the luciferase protein would be possible after crossbreeding the founder mice with a tissue-specific *Cre*-driver mouse.

5 Materials

5.1 Instruments

Instruments	Company
ABI Prism 3730 DNA Analyzer	Applied Biosystems
BD™ CARV II	BD Biosciences
blot system Power Pack P25T	Biometra
Centrifuge 5804 R	Eppendorf
CTI Controller 3700 digital	PeCon
gel electrophoresis chamber Horizon® 11.14	Life technologies
Leica DMI3000 B	Leica
Mastercycler® gradient	Eppendorf
microwave	Bosch
power source PowerPac™ Universal	BioRad
RT3™ Monochrome camera	SPOT™ Imaging Solutions
shaker	New Brunswick Scientific
spectrophotometer Heliosα	Thermo scientific
spectrophotometer NanoDrop	Thermo Fisher Scientific
tempcontrol 37-2 digital	PeCon
Universal Shaker SM 30	Edmund Bühler Johanna Otto GmbH
UV radiator TFX-35 M	Maxilum
vortexer	Janke & Kunkel IKA® Labortechnik
Wallac Victor2 1420 Multilabel Counter	Perkin Elmer
water purification system Milli-Q_{PLUS} PF	Millipore
waterbath Ecoline Star edition	Lauda

5.2 Chemicals

Chemicals	Company
ABI PRISM BigDye Terminator Kit v1.1	Applied Biosystems
ADP	Sigma-Aldrich
agarose MP dry	Roche
ammonium peroxide sulfate (APS)	Sigma-Aldrich
ampicillin	Sigma-Aldrich
ATP	Sigma-Aldrich
Bright-Glo™ Luciferase Assay	Promega
Brij-35	Thermo Scientific
bromophenol blue	Sigma-Aldrich
BSA	New England Biolabs
Complete Mini™	Roche
Coomassie Brilliant Blue G-250	New England Biolabs
coumaric acid	Sigma-Aldrich
dithiothreitol (DTT)	Applichem
ddNTPs fluorescence-marked	Promega
dNTPs	Promega
Dulbecco's Modified Eagle Medium High Glucose (DMEM)	Gibco Invitrogen Promega

DMEM High Glucose, serum-free	Gibco Invitrogen
EDTA pH 8.0	Gibco Invitrogen
EGTA pH 8.0	Carl Roth
ethanol 70%	Merck Darmstadt
ethidium bromide	Carl Roth
fetal bovine serum	Carl Roth
GlutaMAX™ Minimal Essential Medium (MEM)	Gibco Invitrogen
glycerine	Carl Roth
glycerol	Gibco Invitrogen
β-glycerophosphate	Sigma-Aldrich
glycin	Sigma-Aldrich
H_2O_2	Merck Darmstadt
isopropanol	Merck Darmstadt
K_3PO_4	Carl Roth
kanamycin	Carl Roth
lysogeny broth (LB) agar dry	Roth
LB medium dry	Roth
Lipofectamine™ 2000 Transfection Reagent	Invitrogen
luciferin	Life technologies
luminol	Sigma-Aldrich
Magnesium Chloride Solution	Promega
$MgCl_2$	Promega
β-mercaptoethanol	Gibco BML
methanole	Merck Darmstadt
milk powder	Carl Roth
NaCl	Carl Roth
nitrogen	Carl Roth
Nonidet P40 Substitute	Roche
oligomers	Roche
polyacrylamide	Bio-Rad
QIAGEN HiSpeed Plasmid Maxi Kit	MWG-Biotech AG
QIAPrep® Spin Miniprep Kit	QIAGEN
QIAquick Gel Extraction Kit	QIAGEN
QIAquick PCR Purification Kit	QIAGEN
Sephadex™ G50	GE Healthcare
sodium deoxycholate	Fluka
sodium dodecyl sulfate	Merck
tetramethyldiamine	Merck
Tris-Base	Merck
Tris-HCl	Merck

5.3 Consumables

Consumables	Company
cell culture dishes 60 cm²	BD Bioscience
comb	Hoefer
cuvette 1.5 ml	Hellma
Falcon reaction tubes	BD Bioscience
forceps	World Precision Instruments
glass cylinder	Schott
glass plates	Menzel Braunschweig
insuline syringe 1 ml	Terumo
microtiter plate, black	Thermo Fisher Scientific
nitrocellulose membrane	PROTRAN® Th.Geyer
object holder	Menzel Braunschweig
petri dish	BD Bioscience
pipet	Eppendorf
pipet tips	VWR
pipette boy	Integra
reaction tube (1.5 ml)	Eppendorf
reaction tube with screw cap	VWR
Tween 20	Applichem
Whatman® Paper	Biometra
Xray film Super RX	FUJIFILM Europe

5.4 Length standards

Length standard	Company
DNA marker TrackIt™ 1 kbp DNA ladder	Invitrogen
DNA marker TrackIt™ 100 bp DNA ladder	Invitrogen
PageRuler™ Prestained Protein Ladder	Fermentas

5.5 Restriction endonucleases and other enzymes

Enzyme	Company
exonuclease I	New England Biolabs
Gateway® Recombination System	Invitrogen
restriction enzymes	New England Biolabs
restriction enzyme digestion buffers	New England Biolabs
PCR buffer 5x Colorless GoTaq™ PCR buffer	Promega
PCR buffer 5x Green GoTaq™ PCR buffer	Promega
Phusion® High-Fidelity DNA polymerase	Finnzymes
Phusion® High-Fidelity polymerase buffer 5x	Finnzymes
2x Rapid Ligation Buffer	Promega
shrimp alkaline phosphatase	Roche
T4 DNA Ligase	Promega
Taq polymerase GoTaq™ DNA Polymerase	Promega

5.6 Oligonucleotides (primers)

For amplification, cloning and sequencing, all oligonucleotides were custom-ordered from *Eurofins MWG*.

Primer N°	Sequence (5'-3')	Primer function
S2381	CTAGCAAAATAGGCTGTCCC	forward, pre-*luc* sequence of pGL3-basic
S2382	GACGATAGTCATGCCCCGCG	reverse, pre-*luc* sequence of pGL3-basic
S2383	CGTTTCATAGCTTCTGCCAAC	reverse, within *luc* sequence
S2390	GGTGGTAGATCTTCGAAGGAGATAGAAC-CATGTCTGTCCTGACGCCACT	forward, designed primer, first six amino-acids of *Cox8a*
S2391	GGTGGTAAGCTTTCTTATCGTCGT-CATCCTTGTAATCCTCCCGCGCCGGCTTCG AGT	reverse, designed primer, last six amino acids of *Cox8a*
S2458	TCGTTGCAACAAATTGATAAGC	forward, attL1-site of pENTR1A-DS
S2459	GGCTTCGAGTGGACCTGAG	reverse, *Cox8a* sequence
S2460	GGAAAACTCGACGCAAGAAA	forward, within *luc* sequence
S2462	CGGAATGCCAAGCTTTCTTA	reverse, within *cox8a-flag-luc* sequence between *flag* + *luc*
S2587	TAATACGACTCACTATAGGG	forward, "T7 primer" site of pcDNA3.2/V5-DEST
S2588	ATACCGTCGACCTCGAATCA	forward, pre-insert of pROSA26_cox8a-flag-luc
S2592	GATGGCTGGCAACTAGAAGG	reverse, post-attB2-site of pROSA26_cox8a-flag-luc

5.7 Plasmids and bacterial strains

Vector	Size	Company
pcDNA™3.2/V5-DEST	7,711 bp	Invitrogen
pENTR1A_DS	3,754 bp	Invitrogen
pGL3-basic	4,818 bp	Addgene
pROSA26-DEST	14,820 bp	Addgene

Bacterial strain	Company
One Shot® ccdB Survival Cells	Invitrogen
One Shot® TOP10 Competent Cells	Invitrogen
S.O.C. medium	Invitrogen

5.8 Cell lines

Cell line	Company
COS1 cells	ATCC
HEK293 cells	ATCC

5.9 Antibodies

Antibody	Company
Alexa Fluor® 488 goat anti-mouse IgG	Invitrogen
anti-beta Tubulin rabbit polyclonal antibody	abcam 6046
ANTI-FLAG® M2 Antibody	Agilent Technologies Genomics
goat-anti rabbit IgG /POD	Merck

5.10 Buffers, solutions, and media

Solution	Composition
PBS (10x), PH 7.4	1.4 NaCl, 27 mM KCl, 81 mM Na_2HPO_4 x H_2O, 15 mM KH_2PO_4
TE buffer (1x), pH 7.4	10 mM Tris, 1 mM Na_2-EDTA
TBE buffer (5x), pH 8.0	0.5 M Tris-HCl, 0.5 M boric acid, 10 mM Na_2-EDTA

Bacterial stem medium	Composition
culture medium	tryptone 10 g/l, yeast extract 5 g/l, NaCl 5 g/l, ampicillin 125 mg/ml
S.O.C. medium	2% tryptone, 0.5% yeast extract, 10 mM NaCl, 2.5 mM KCl, 10 mM $MgCl_2$, 10 mM $MgSO_4$, 20 mM glucose

Cell medium	Composition
growth medium COS1 cells	DMEM 500 ml, fetal bovine serum 10%
growth medium HEK293 cells	DMEM 500 ml, fetal bovine serum 10%, 0.5x GlutaMAX™ I

Protein extraction buffer	Composition
lysis buffer	10 mM K_3PO_4, 1 M $MgCl_2$, 50 mM β-glycerophosphate, 0.5 M EDTA pH 8.0, 0.5 M EGTA pH 8.0, 10% Brij-35, 5% sodium deoxycholate, 1 M DTT, 10% Nonidet P40 Substitute, 1 tablet Complete Mini™ per 10 ml lysis buffer

SDS-PAGE buffer	Composition
4x lower buffer	1.5 M Tris-HCl pH 8.8, 0.4% SDS
4x upper buffer	0.5 M Tris-HCl pH 6.8, 0.4% SDS
1x loading buffer	25 mM Tris-Base, 192 mM glycin, 1% (w/v) SDS
2x sample buffer	62.5 mM Tris-HCl pH 6.8, 25% (v/v) glycerine, 2% (w/v) SDS, 350 mM DTT, 0.025% (w/v) bromophenol blue

SDS-PAGE gel	Composition
separating gel	1x lower buffer, 10% (v/v) PAA (29:1), 0.1% (v/v) APS, 0.1% (v/v) TEMED, ddH_2O
stacking gel	1x upper buffer, 5% (v/v) PAA (29:1), 0.1% (v/v) APS, 0.1% (v/v) TEMED, ddH_2O

Western Blot solution	Composition
blot buffer	1x Laemmli buffer, 30% (v/v) methanol
blocking solution	5% BSA, 20 mM Tris-HCl pH 7.5, 150 mM NaCl, 0.05% Tween 20
incubation solution	5% (w/v) milk powder, 20 mM Tris-HCl pH 7.6, 150 mM NaCl, 0.05% Tween 20
washing buffer	20 mM Tris-HCl pH 7.5, 150 mM NaCl, +/- 0.05% Tween
ECL solution A	0.1M Tris pH 8.3, 0.4 mM coumaric acid, 2.5 mM luminol
ECL solution B	0.1 M Tris pH 8.3, 0.018% (v/v) H_2O_2
stripping solution	Rotifree Stripping Buffer: 62.5 mM Tris-HCl pH 6.8, 2% (w/v) SDS, 0.7% β-mercaptoethanol

5.11 Software

Program	Company
DNASTAR Lasergene® 8	DNASTAR
ImageJ	Wayne Rasband, National Institutes of Health
Image-Pro Plus	MediaCybernetics
MS Office	Microsoft
Primer3	Steve Rozen, Helen Skaletsky[72]
Vector NTI® Software	Invitrogen

6 Methods

6.1 Molecular biological methods

6.1.1 Polymerase Chain Reaction

Polymerase Chain Reaction (PCR) allows amplifying short DNA sequences by means of cyclic reaction temperature changes.[73,74] The length and sequence of the DNA template as well as the length and sequence of the primers influence different parameters of a PCR, as for example the annealing temperature and the elongation time. An exemplary PCR protocol is shown in Figure 6, a standardized reaction assay is shown in Figure 7.

Phase	Temperature [°C]	Duration	Number of cycles
denaturation	96	3 min	1
denaturation **annealing** **elongation**	96 60 72	30 s	 30
final elongation	72	3 min	1

Figure 6: Example of a PCR protocol. In the text, the single steps are indicated as followed: denaturation = denat, annealing = ann, elongation = elong.

Chemicals	Volume [µl]	Note
buffer	10.0	contains a final concentration of 1.5 mM $MgCl_2$
dNTPs	0.5	200 µM per nucleotide
$MgCl_2$	5.0	0.5-2.5 mM
forward primer	0.5	5 pmol
reverse primer	0.5	5 pmol
Taq DNA polymerase	0.2	1 U
DNA template	1.0	variable according to concentration
ddH_2O	32.3	variable according to DNA volume
sum	50.0	

Figure 7: Standardized PCR reaction assay.

6.1.2 Restriction enzyme digestion

Restriction enzyme digestion is based on the use of restriction endonucleases that are able to cut double stranded DNA at specific recognition sites. The process results in two compatible ends that can be fused again by a ligation reaction. The method of restriction enzyme digestion is employed either for diagnostics or for preparation of cloning fragments. In order to insert a DNA sequence into a plasmid, one has to cleave the sequence and the plasmid with the same restriction endonucleases and ligate them. Some restriction enzymes need bovine serum albumin

(BSA) for stabilization.[75] To prevent self-ligation of the free ends, it is recommended to perform a dephosphorylation of the vector backbone before the ligation reaction. The nomenclature of the restriction enzymes used here conforms to the recommendations of Roberts *et al.*.[76]

6.1.3 Ligation

During a ligation reaction, the gap between the 5'-phosphate group of one end of a DNA strain and the 3'-OH group of the other end is closed into a covalent bond. This is done by means of a DNA ligase.[77–81] This reaction is part of the process of DNA replication or splicing in eukaryotic cells. It was used since the early days of transgenic techniques to ligate free DNA ends after a restriction enzyme digestion.

6.1.4 Sequencing

In the process of multi-step cloning it is desirable to control the correctness of the DNA sequence between the single cloning steps. The most reliable method is automatic DNA sequencing. In this context, we chose the chain-termination method by Sanger.[82] This is an amplification method using a certain number of dideoxynucleotide triphosphates (ddNTPs) in addition to the deoxynucleotide triphosphates (dNTPs) usually applied for a PCR. The ddNTPs lack a 3'-OH-group that is required for the formation of a phosphodiester bond between two nucleotides, hence the integration of a ddNTP leads to chain termination. Smith *et al.* presented a method using fluorescently labelled ddNTPs.[83] The incorporation of four fluorophores with different emission wavelengths, according to the four different base-specific reactions, allows analyzing the DNA fragments in a single gel electrophoresis run. Slab gel electrophoresis is now replaced by capillary electrophoresis, a technique primarily presented by Jorgensen *et al.* in 1981.[84] Sequencing was performed by means of the *ABI Prism 3730 DNA Analyzer*. I used the program *DNASTAR® Lasergene8 Seqman* for the analysis of the sequences.

6.1.5 Gel electrophoresis

I used gel electrophoresis to verify the result of either a PCR or restriction enzyme digestion. For an agar gel, I dissolved 0.8 to 1.5 g agarose in 100 ml Tris base, boric acid, EDTA (TBE) buffer. The running time and voltage differed according to the expected length of the loaded DNA sample. Visualization was done on an UV tray in a closed device with an integrated camera. Finally, I determined the length of the DNA fragments by comparison with a co-loaded DNA molecular weight marker. Whenever extraction of the DNA fragment from the gel was necessary, I used the *QIAquick Gel Extraction Kit* according to the protocol of the manufacturer.

6.2 The Gateway® Recombination System

The ***Gateway® Recombination System*** is based on the site-specific recombination pathway of the bacteriophage *lambda* in order to simplify the cloning process. The bacteriophage *lambda* possesses a sequence called *att*P (P for phage), the *E. coli* genome contains a DNA sequence called *att*B (B for bacterial cell). After infection, the two corresponding sites are brought close together and the recombination takes place by means of the phage-encoded protein integrase and the host-encoded protein integration host factor. The result is the integration of the phage DNA into the bacterial genome. Afterwards, the phage DNA is flanked by *att*L (L for left) and the *att*R (R for right), both hybrids of *att*P and *att*B. The reverse reaction happens between *att*L and *att*R and results in the excision of the phage DNA and the reconstitution of the original *att*B and *att*P sequences.

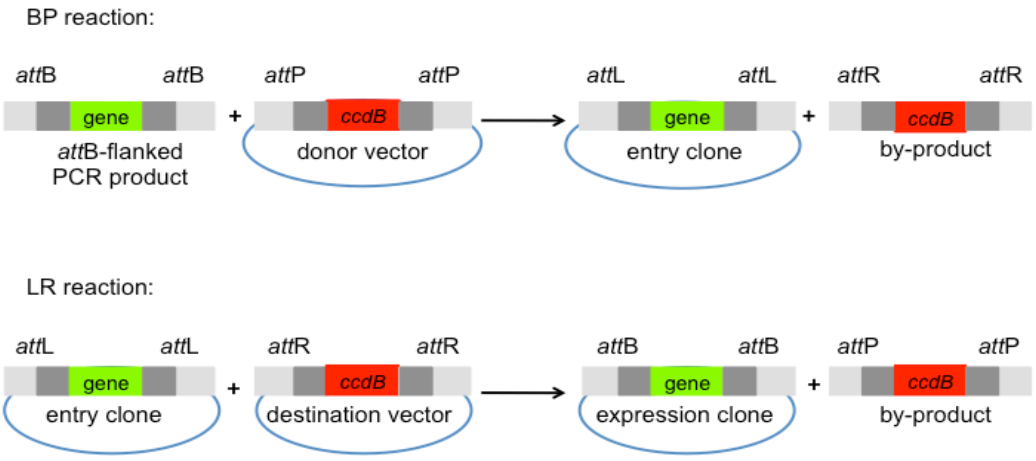

Figure 8: The *Gateway® Recombination System* reactions.

This principle was adapted for molecular cloning: different vectors contain a specific, modified *att* site (Figure 8). They act as complementary pairs. The sequence of interest needs to be flanked by *att*B sites. The basic plasmid (donor vector) has *att*P sites and the sequence of the *ccdB* gene. The *ccdB* (ccd for control of cell death) gene encodes for a lethal toxin. The toxin CcdB is part of the CcdA/CcdB II toxin-antitoxin system.[85,86] The target of the protein CcdB toxin is a subunit of the bacterial gyrase, an essential enzyme of *E. coli*, comparable to type II topoisomerase. *E. coli* strains that host a plasmid coding for the CcdB toxin do not survive. Therefore, vectors containing the *ccdB* gene need to be propagated in *E. coli* strains resistant to the CcdB toxin. The *Gateway® Recombination System* makes use of the CcdB toxin. After the first recombination reaction, the gene of interest is integrated into the basic plasmid (now called **entry clone**). Cells containing the entry clone and hence the gene of interest proliferate, whereas cells that take up

the by-product with the *ccdB* gene fail to grow. This first reaction is termed BP reaction, as the recombination takes place between *att*B and *att*P sites. The next step is the LR reaction between the entry clone with *att*L sites and the destination vector with *att*R sites. The gene of interest is transferred from the entry clone into the **destination vector**. There are two different enzyme mixtures that catalyze the reactions. The *BP Clonase™* reagent contains the bacteriophage *lambda* integrase and the *E. coli* integration host factor. For the *LR Clonase™* enzyme mix, the enzyme bacteriophage *lambda* excisionase is added.[87] The entry clone is the versatile element of the *Gateway® Recombination System*, it is compatible with numerous vectors adapted for different expression systems, as for example *E. coli*, mammalian cells, yeast, insects. Beside the recombination sites *att*R, each vector contains the elements needed for expression of the gene of interest in the particular expression system.

6.3 Cloning

6.3.1 Transformation

Transformation of *E. coli* was performed according to Cohen and coworkers.[88] I purchased heat-shock competent *E. coli* JM109 cells from Promega. Cells were thawed, mixed with the plasmid and heat-shocked at 42°C for 2 minutes to facilitate the uptake of DNA. The incubation in SOC medium at 37°C followed before plating on agar plates with the selective antibiotics. Colonies grew overnight at 37°C.

6.3.2 Overnight culture

Before extracting plasmid DNA from transformed bacterial cells, they have to reach the highest possible optical density. I incubated the suspension of transformed bacterial cells overnight at 37°C in an orbital shaker at 225 rpm. The container that holds the medium with the cells had a fivefold higher volume than the volume of the medium. This treatment ensures the optimum O_2 supply necessary for a high growth rate.

6.3.3 DNA preparation

The DNA isolation was done with commercial kits of QIAGEN according to the instruction manual. For analysis of the isolated DNA (mini-preparation), the *QIAPrep® Spin Miniprep Kit* was used. The principle of the kit is based on alkaline lysis of bacterial cells, followed by filtration of the DNA by binding to a silica gel membrane.[89] The method of maxi-preparation by means of *QIAGEN HiSpeed Plasmid Maxi Kit* yielded a large amount of a very pure plasmid DNA. Again, the isolation started with alkaline lysis. DNA was here adsorbed to an anion-

exchange resin. After washing, the DNA was eluted in a high-salt buffer and precipitated by iso-propanol. DNA concentration was analyzed with a micro-spectrophotometer (*NanoDrop*).

6.4 Vector construction

6.4.1 pGL3_cox8a-flag-luc

The pGL3-basic plasmid (Figure 9) was grown in JM109 cells in LB-medium using 125 mg/ml ampicillin selection and preparation was done as described above. I verified the presence of the insert by PCR using the primer combinations S2381/2382 and S2460/2382. Next, I digested the vector pGL3-basic in order to prepare it for ligation (Figure 10).

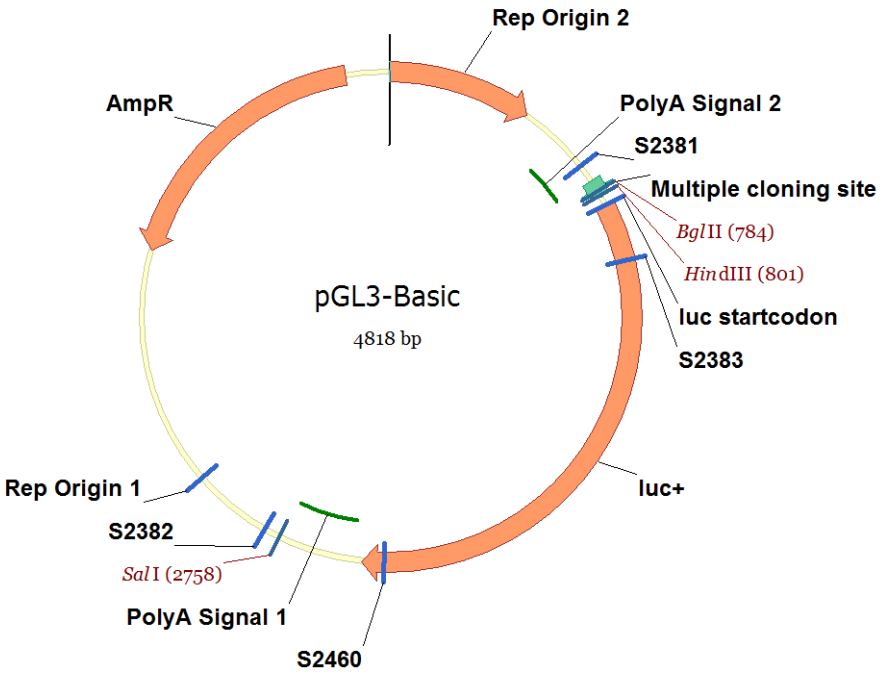

Figure 9: The pGL3-basic vector containing the *luc* gene.

Components	Amount	Volume [µl]
pGL3-basic	230 ng	2
*Bgl*II	20 U	2
*Hind*III	20 U	1
Buffer 2 (10x)	4 µl	4
H_2O HPLC	31 µl	31
sum		40

Figure 10: Protocol for the restriction enzyme digestion of the pGL3-basic plasmid. The reaction mixture was incubated at 37°C for 1 h, then incubated at 65°C for 20 min for restriction enzyme inactivation.

I amplified the ***Cox8a* import sequence** from mouse liver cDNA (Figure 11). The forward primer annealed to the first 18 coding nucleotides of mouse *Cox8* and at its 5'-end a *Bgl*II restriction site was introduced, followed by the Shine-Dalgarno sequence (Figure 12). The Shine-Dalgarno sequence is necessary for translation in prokaryotes.[90] The eukaryotic start codon is embedded in the Kozak consensus sequence, which is obligatory for DNA translation in eukaryotes.[91] The reverse primer included the base pairs encoding the last six amino acids of the gene and the FLAG™-epitope and a *Hind*III restriction site at its 5'-end.[92,93]

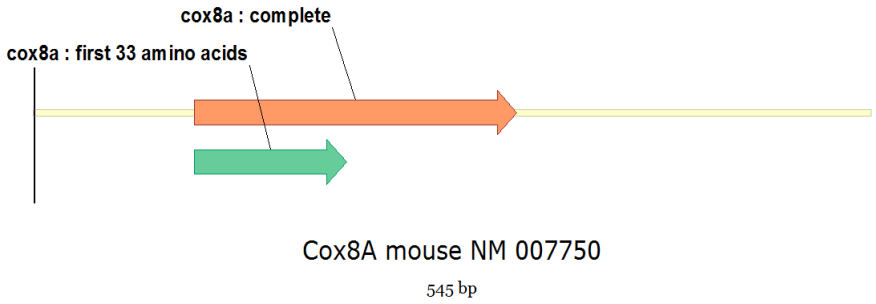

Figure 11: cDNA obtained from mouse liver as template for *Cox8a*.

Forward primer:

5-GGTGGTAGATCTTCGAAGGAGATAGAACCATGTCTGTCCTGACGCCA-3

- 5' overhang
- restriction site for *Bgl*II
- Shine-Dalgarno
- Kocak sequence
- **first 18 coding bp of *Cox8a***

Reverse primer:

5-GGTGGTAAGCTTTCTTATCGTCGTCATCCTTGTAATCCTCCCGCGCCGGCTTCGAGT-3

- **last 18 coding bp of *Cox8a* import sequence**
- FLAG™ tag + termination codon
- restriction site for *Hind*III
- 5' overhang

Figure 12: Primer design for amplification of the *Cox8a* sequence.

I amplified the fragment using the proofreading polymerase *Phusion® High-Fidelity DNA polymerase* in order to prevent the insertion of mutations by PCR. The resulting sequence was then digested with the restriction enzymes *Bgl*II and *Hind*III at 37°C for 1 h, followed by 20 min inactivation at 65°C. I separated the restriction products on a 1.5% agarose gel and the 147 bp band was purified with the *QIAquick Gel Extraction Kit*. For ligation, I chose a molar insert:vector ratio of 1:3 and the protocol detailed in Figure 13.

	Amount	Volume [µl]
pGL3-basic digested	45.1 ng	11
cox8a-flag digested	8.8 ng	1
2x Rapid Ligation Buffer		15
T4 DNA Ligase	9 U	3
sum		30

Figure 13: Protocol of the ligation of the digested pGL3-basic vector and the digested insert *Cox8a-flag*.

The ligated plasmid (pGL3_cox8a-flag-luc) was transformed into *One Shot® TOP10 Competent Cells via* heat-shock and grown on agar plates using ampicillin selection. I subsequently checked the clones by colony PCR using the S2381/2383 primer combination. Potentially correct clones were subcloned in LB liquid culture and mini-prepped one day later and verified by automatic Sanger sequencing. Correct clones were stored as glycerol stocks at -70°C.

6.4.2 pENTR1A_DS_cox8a-flag-luc

I transformed *One Shot® ccdB Survival Cells* with 0.5 µg of the vector pENTR1A_DS (Figure 14) according to the protocol. To obtain the plasmid, an overnight culture and a mini-preparation followed. The insert *Cox8a-flag* and the vector pENTR1A_DS were digested in order to prepare their ligation (Figure 15). I chose the four restriction enzymes in such a manner that compatible cohesive ends were created which could not be cut afterwards. The restriction site of *Bgl*II was compatible with the site of *BamH*I, the same for the restriction endonucleases *Sal*I and *Xho*I.

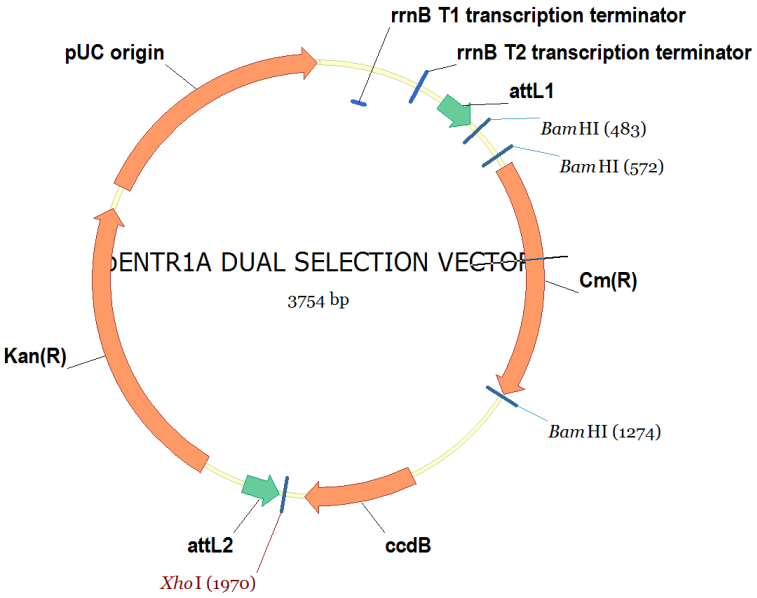

Figure 14: Vector map of the entry vector pENTR1A_DS.

	Amount	Volume [µl]
pGL3-basic_cox8a-flag	1.705 µg	25
*Bgl*II	20 U	2
*Sal*I	20 U	1
Buffer 2 (10x)		4
BSA	4 µg	4
H_2O HPLC		4
sum		40

	Amount	Volume [µl]
pENTR1A_DS	2 µg	20
*BamH*I	20 U	1
*Xho*I	20 U	1
Buffer 3 (10x)		4
BSA	4 µg	4
H_2O HPLC		10
sum		40

Figure 15: Protocols of the REDs of pGL3-basic_cox8a-flag and the entry vector pENTR1A_DS.

The digestion assays were purified on an agarose gel and extracted. The digested plasmid pENTR1A_DS was dephosphorylated using 1U Shrimp Alkaline Phosphatase in conformity with the protocol to prevent self-ligation. The ligation of the digested and dephosphorylated pENTR1A_DS vector with the digested insert *cox8a-flag-luc* was done in a 1:1 ratio (Figure 16). The mixture was incubated for 1 hour.

	Amount	Volume [µl]
pENTR1A_DS digested + dephosphorylated	55 ng	2
cox8a-flag-luc digested	52 ng	4
2x Rapid Ligation Buffer		10
T4 DNA Ligase	3 U	3
sum		20

Figure 16: Protocol of the ligation reaction between pENTR1A_DS and *cox8a-flag-luc*.

The transformation into *One Shot® TOP10 Competent Cells* was carried out according to the supplier's instructions. I selected cells containing the resulting plasmid pENTR1A_DS_cox8a-flag-luc for kanamycin resistance. The success of the ligation was proven by PCR. The primers S2458, S2459 allowed the amplification of one of the two transition sites. The PCR was positive for each of the six clones. I mini-prepped three clones, they were sequence-verified in both orientations.

6.4.3 pROSA26_cox8a-flag-luc

The destination vector for the recombination reaction, pROSA26-DEST, was streaked out on an agar plate and incubated overnight (Figure 17). I chose one of the colonies and inoculated six reaction tubes containing 10 ml LB medium with 125 mg/ml ampicillin. The cells grew overnight while shaking at 37°C and 220 rpm. 800 µl of this solution and 200 µl glycerol were mixed and frozen at -80°C serving as glycerol stocks. From the residual solution, I extracted DNA using the *QIAPrep® Spin Miniprep Kit*. The final concentration was measured with a spectrophotometer. I controlled pROSA26-DEST by digestion with *Kpn*I. This restriction enzyme was destined for linearization of the final plasmid.

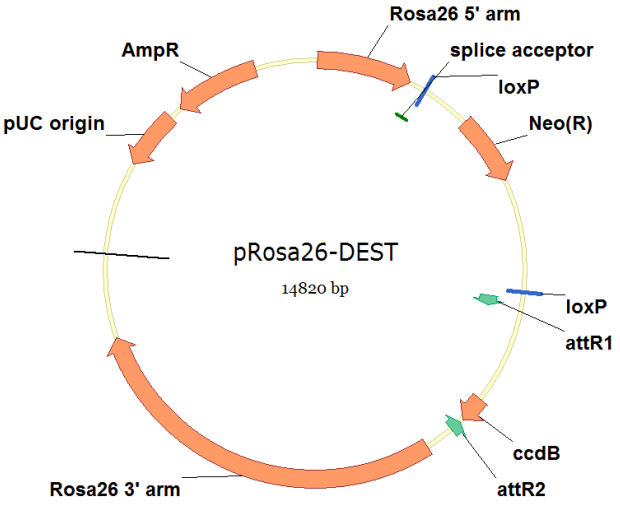

Figure 17: Vector map of the destination vector pROSA26-DEST.

pENTR1A_DS_cox8a-flag-luc was incubated with pROSA26-DEST in an two hour LR recombination reaction using *Gateway® LR Clonase™ II Enzyme Mix* (Figure 18).

	Amount	**Volume [µl]**
pENTR1A_DS_cox8a-flag-luc	150 ng	1
pROSA-DEST	150 ng	1
TE Buffer, pH 8.0		6
LR Clonase™ II Enzyme Mix		2
sum		10

Mixture is vortexed briefly twice and microcentrifuged briefly, then incubated for 2 h at 25°C. Then addition of:

Proteinase K	2 µg	1

Mixture is vortexed briefly, then incubated for 10 min at 37°C.

Figure 18: Protocol of the LR reaction between pENTR1A_DS_cox8a-flag-luc and pROSA-DEST.

One Shot® TOP10 Competent Cells were transformed with the pROSA26_cox8a-flag-luc vector. I selected clones *via* drug resistance and identified correct clones by two colony PCRs primer pairs S2588/S2383 and S2460/S2592. Six clones of pROSA26_cox8a-flag-luc were mini-prepped. I digested two of them by the restriction enzymes *Eco*RI, *Hind*III and *Sal*I to check the size of the resulting plasmid. The plasmid pROSA26_cox8a-flag-luc was produced in high quantity by maxi-prep with the *QIAGEN HiSpeed Plasmid Maxi Kit*. The cells grew in LB medium with ampicillin (100 µg/ml) and were incubated overnight at 37°C with shaking at 225 rpm. To confirm the plasmid used for maxi-preparation, I digested it with *Eco*RI, *Hind*III and *Sal*I under the same conditions.

6.4.4 pcDNA3.2/V5_cox8a-flag-luc

Another LR recombination reaction was performed between pENTR1A_DS_cox8a-flag-luc and pcDNA™3.2/V5-DEST (Figure 19) by incubation at 25°C for one hour. Four clones were mini-prepped, three of them were proven to be correct by PCR with the primer combination S2587/S2462. I controlled two clones of the vector pcDNA3.2/V5_cox8a-flag-luc by restriction enzyme digestion with *Bgl*II. Sequencing was used to finally confirm correct cloning.

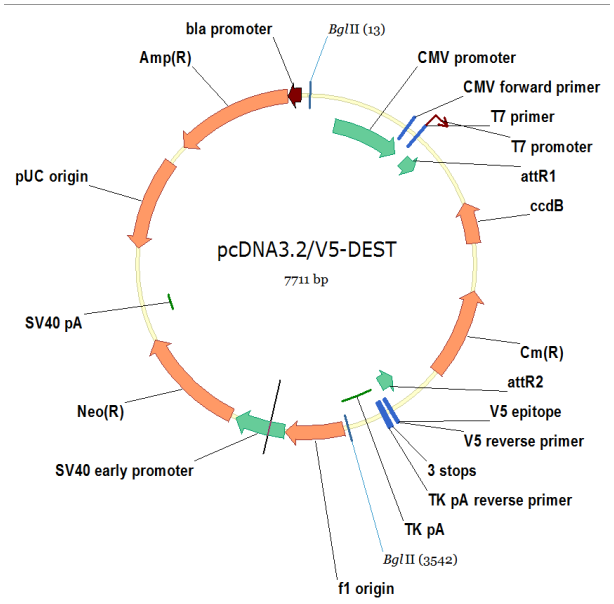

Figure 19: Vector map of destination vector pcDNA3.2/V5-DEST.

6.5 Cell culture methods

I performed cell culture experiments to control the localization of the gene of interest in mitochondria and its ability to convert the substrates luciferin, ATP, magnesium and oxygen to AMP, carbon dioxide and light.

6.5.1 Cell culture

HEK293 cells and COS1 cells grew in growth medium in a 5% carbon dioxide (CO_2) atmosphere. HEK293 cells demand Dulbecco's Modified Eagle Medium (DMEM) High Glucose, 10% fetal bovine serum and 0.5x *Glutamax*. The growth medium applied to the COS1 cells contained the same ingredients except *Glutamax*. The medium was changed three times a week.

6.5.2 Transfection

A transient transfection of both cell lines with the plasmid pcDNA3.2/V5_cox8a-flag-luc was done by lipofection. DNA and *Lipofectamine™ 2000 Transfection Reagent* were mixed at a ratio of 1:3. For every well, 0.8 µg of pcDNA™3.2/V5_cox8a-flag-luc was added to 100 µl serum-free DMEM High Glucose. 2.4 µl of *Lipofectamine™ 2000 Transfection Reagent* was diluted in 100 µl serum-free DMEM High Glucose. After five minutes, I mixed both solutions and the assay rested at room temperature for 20 minutes. The cells were incubated in the transfection solution for 24 h at 37°C with 5% CO_2.

6.5.3 Luciferase assay

A luciferase assay is performed with transgenic cells that express the protein firefly luciferase. The emitted light is detected by a luminometer, an instrument for the measurement of light emission. Microtiter plate luminometers allow a simultaneous detection of different assays. Most luminometers count the number of photons with a photomultiplier as Relative Light Units (RLU).[63]

I performed three different luciferase assays, which all started with transfection of cells with pcDNA3.2/V5_cox8a-flag-luc via *Lipofectamine™ 2000* (see 6.5.2). Different substrates were added under aerobic conditions: *Bright-Glo™ Luciferase Assay Reagent*, luciferin, ADP, or ATP. I measured the light emission by means of the *Wallac Victor2 1420 Multilabel Counter* and statistically analyzed the resulting data with *Microsoft Office Excel*.

[1] The assay included transfected and non-transfected **COS1** and **HEK293 cells**. Non-transfected cells were also treated with the transfection mixture, but no DNA was supplied. Test cells were transfected with 0.4 µg DNA. 100 µl fresh medium and 100 µl *Bright-Glo™ Luciferase Assay Reagent* per well were added at room temperature for two minutes until the cells were lysed. I transferred 200 µl/well of the mixture to a well of a black microtiter plate. I analyzed three samples of each composition and I repeated the measurement four times.

[2] About 3,000 **COS1 cells** per well were seeded and the cells of half of the wells were transfected with 0.1 µg DNA. First, 500 µM ADP were added as a substrate. Then I added the sub-

trate **luciferin** in increasing amounts of 500 µM, 1,000 µM and 2,000 µM to three wells of transfected and non-transfected cells. These samples were measured 94 times. Cells with the mixture *Bright-Glo™ Reagent* added were tested as controls. Every measurement was repeated ten times. **[3]** A set of transfected and non-transfected **COS1 cells** was supplied with 500 µM luciferin, 500 µM ADP and 5 mM malate and glutamate each. Both are substrates of the malate-aspartate-shuttle system and necessary for electron transport from the cytosol to the mitochondrial matrix through the intramitochondrial membrane that is impermeable to $NADH_2$. $NADH_2$ is the most important reducing equivalent that supplies the respiratory chain with electrons. The cells are recharged with either 500 µM luciferin or 500 µM ADP and **measured again after 20 minutes**.

6.5.4 Immunofluorescence

Fluorescence is the emission of light by a substance after having absorbed energy through one or more photons. The components of molecules causing fluorescence are called fluorophores. This functional group can absorb a photon of a certain wavelength and energy by which it is excited to a higher energy level. By falling back into its ground state, the fluorophore emits light of a longer wavelength and therefore lower energy. This change of wavelength is named Stokes shift, after its discoverer Sir George Stokes.[94]

Immunofluorescence is the visualization of certain components of a cell or tissue based on antibody-antigen interaction. The fluorophore is bound to an antibody that recognizes a defined target, its specific antigen. It detects the distribution of proteins, glycans and other small molecules within a cell, a cell culture or a tissue section.

The method of immunofluorescence can be combined with other fluorescence techniques on the same sample to demonstrate co-localization of two (or more) targets. Two fluorescent substances that are not based on antibody-antigen interactions are 4,6-diamidino-2-phenylindole (DAPI) to stain DNA and *MitoTracker*® to stain mitochondria. DAPI attaches predominantly to double-stranded DNA and can permeate the cell membrane of living cells.[95] *MitoTracker*® is a lipophilic cationic dye that binds covalently to mitochondrial proteins.[96] Visualization by a microscope can distinguish the different cell compartments by means of the different colours of the emitted light. Often, a fluorescence microscope is combined with a confocal system. It allows a better resolution and three-dimensional reconstruction by "optical sectioning".

Cells were incubated in fresh medium supplemented with 250 nM *MitoTracker® CM-H_2TMRos* for 45 minutes at 37°C. After washing, the cells were fixed in 4% paraformaldehyde (PFA) for 15 minutes. After permeabilization with 0.5% *Triton X-100* in PBS for 10 minutes, the cells were blocked in 10% horse serum and incubated with the first antibody (*ANTI-FLAG® M2 Antibody*

1:200). After washing, the cells were incubated with the secondary antibody (*Alexa Fluor® 488 goat anti-mouse IgG*, 1:200). After counterstaining with DAPI (1:1,000), the cells were embedded in *Mowiol*.

6.6 Protein biochemical methods

6.6.1 Bradford assay

Protein concentrations were measured with the **Bradford assay**,[97] which is based on the dye *Coomassie Brilliant Blue G-250* that absorbs light at λ=465 nm. Upon binding to protein, its absorption peak shifts to λ=595 nm which can be determined photometrically. The protein concentration in the sample is determined by comparison with a standard dilution series made from bovine serum albumin.[97]

Protein was extracted from HEK293 cells through homogenization in lysis buffer and the sample was centrifuged for 20 minutes at 14,000 rpm at 4°C. 15 µl of the supernatant were used for the Bradford assay and the rest temporarily stored at -80°C.

6.6.2 SDS-PAGE

Proteins in the sample were separated by **Sodium Dodecyl Sulfate Poly-Acrylamide Gel Electrophoresis (SDS-PAGE)**. In this process, the proteins form negatively charged complexes with SDS that run in an electrical field according to their molecular size and can thus be separated.

The protein was mixed with "Laemmli" loading buffer (Figure 20) and incubated at 95°C for 5 minutes to induce denaturation and then cooled on ice for two minutes. It was loaded onto the SDS-polyacrylamide gel. The gel ran with 40 mA at 4°C for the first hour, then the current was increased to 65 mA for another two hours.

	c [µg/µl]	V for 50 µg [µl]	V 2x sample buffer [µl]	Final V [µl]
HEK293 transfected 8:13 ratio	6.2	8.1	8.1	16.0
HEK293 non-transfected	13.8	3.65	3.65	7.3

Figure 20: Protocol for the extracted protein and loading buffer for SDS-PAGE.

6.6.3 Western blot

Western blot is a method to visualize proteins. The method is based on the electrotransfer of proteins from an SDS-PAGE to a nitrocellulose membrane, where they become accessible, can be marked by specific antibodies, and visualized by corresponding secondary antibodies which carry a fluorophore or an enzyme that catalyzes a color (alkaline phosphatase) or light emitting

(horseradish peroxidase) reaction. The loading of the Western blot can be normalized by the intensity of the band deriving from so-called "housekeeping" proteins such as β-actin, heat-shock protein-90 (Hsp90), glyceraldehyde 3-phosphate dehydrogenase (GAPDH), and α-tubulin.[98]
The protein was transferred onto the membrane with a current of 2 mA per cm^2 for 2.5 hours. The membrane was blocked in milk powder and incubated first with the *ANTI-FLAG® M2* antibody (1:1,000), and then with the secondary *horseradish-marked goat anti-mouse IgG* antibody (1:2,000). Visualization of the membrane was done by the enhanced chemiluminescence light (ECL) reactions and recorded on photographic film plates. Anti-beta Tubulin rabbit polyclonal antibody (1:12,500) was used for loading control.

6.7 Generation of transgenic, chimeric mice

The vector pROSA26_cox8a-flag-luc was later transfected into mouse embryonic stem cells by a commercial company. After homologous recombination with the ROSA-locus, these cells were used for blastocyst injection. Transgenic mice could be successfully generated that were able to pass the transgene to their offspring. This work, however, was not part of my dissertation project.

7 Results

The aim of my work was to clone a vector containing the *luc* gene for the generation of a mito-ATP sensitive transgenic mouse. In order to target the protein luciferase to the mitochondria, the *Cox8a* precursor sequence was needed. The FLAG™ tag was added as a means of verifying the localization within a cell. Common molecular genetic methods were applied, such as PCR, restriction enzyme digestion, dephosphorylation, ligation, electrophoresis, sequencing, translation, and mini- and maxi-preparation. The combination of the different gene sequences was facilitated by means of the *Gateway® Recombination System* (Figure 21). Cell culture experiments with subsequent immunostaining allowed verification of the correct targeting of the transgene to the mitochondria and the functionality of the luciferase gene within the mitochondria.

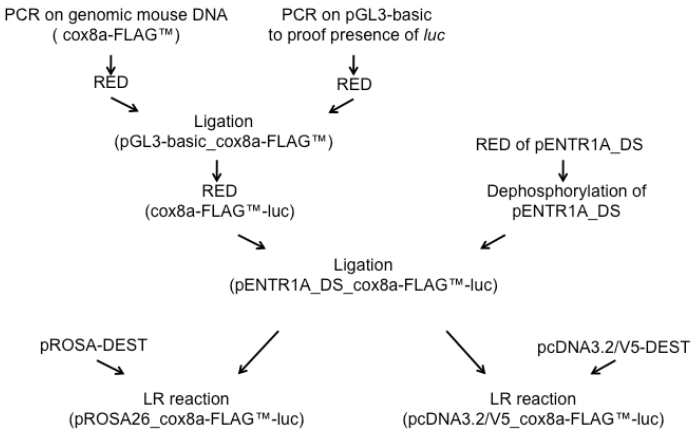

Figure 21: Flowchart of the single steps of vector construction.

7.1 Molecular biological methods

7.1.1 The pGL3-basic vector

The pGL3-basic vector was cultured in *E. coli* JM109 cells and DNA extracted by miniprep (Quiagen). After restriction enzyme digestion with *Hind*III and *Bgl*II, the 4801 bp fragment containing the vector backbone and the luciferase (*luc*) gene was purified by gel electrophoresis. The presence of the *luc* gene was verified by PCR with the primers S2381/S2383 by which I obtained a 352 bp product (Figure 22).

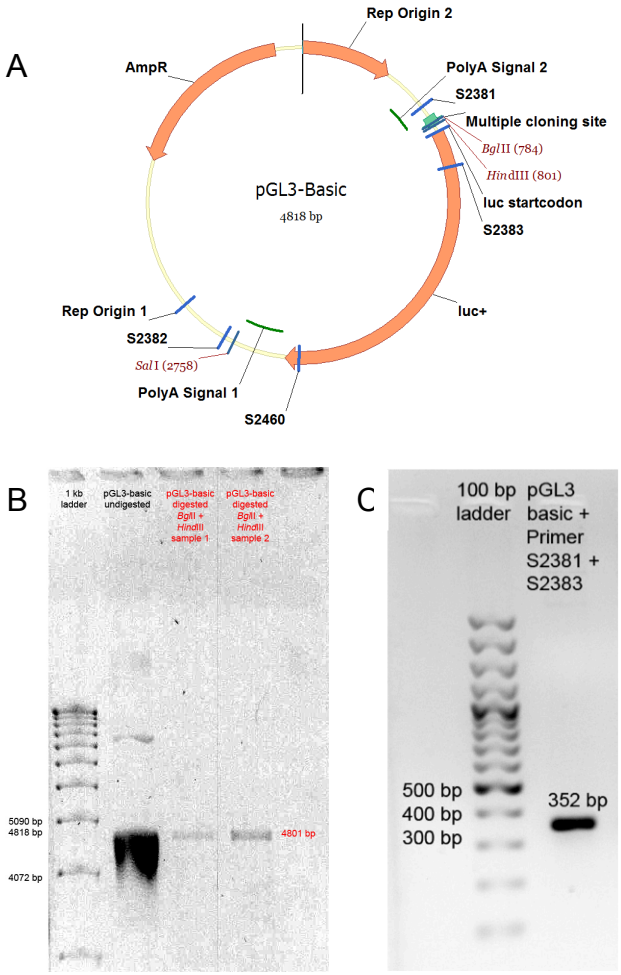

Figure 22: Proof of presence of the *luc* gene. (A) Vector map of pGL3-basic. (B) Purified plasmid backbone + *luc* on agarose gel electrophoresis. (C) Gel electrophoresis of the PCR fragment generated with *luc* specific oligonucleotide primers.

7.1.2 The *Cox8a-FLAG* insert

I performed a PCR on genomic DNA of mouse liver in order to amplify the mitochondrial targeting sequence *Cox8a*. During the amplification process, the sequences of the restriction enzymes sites of *Bgl*II and *Hind*III, of the Shine-Dalgarno sequence, of the Kozak consensus sequence and of the FLAG™ tag were artificially inserted *via* the oligonucleotide primers (Figure 23). The successful integration of these parts is shown *via* gel electrophoresis. After PCR purification, the *Cox8a-flag* sequence was digested with *Bgl*II and *Hind*III to fit it into the digested pGL3-basic plasmid (Figure 24).

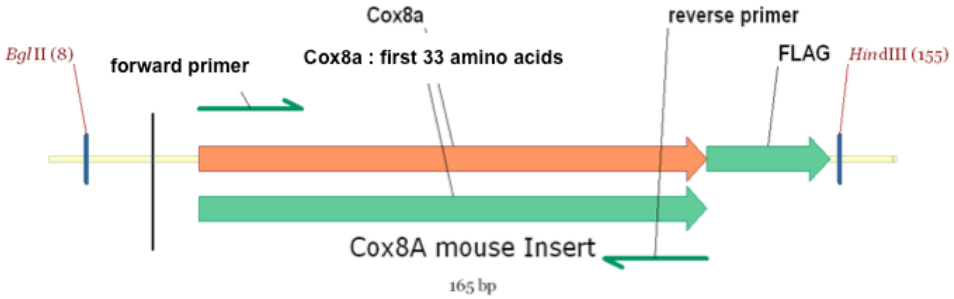

Figure 23: Cloning of the fragment cox8a-FLAG™. Fragment *Cox8a-flag* after PCR on genomic mouse DNA with designed primers.

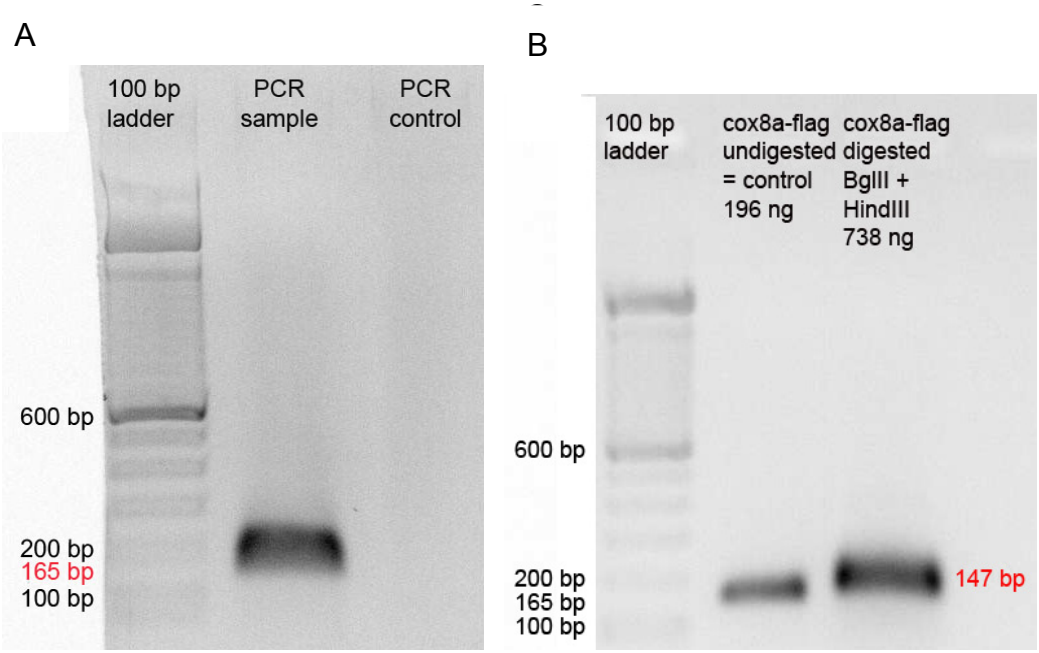

Figure 24: Cloning of the fragment cox8a-FLAG™. (A) Gel electrophoresis of *Cox8a* PCR products from genomic mouse DNA with designed primers. The expected sequence is 165 bp long. (B) Gel electrophoresis after restriction enzyme digestion with *Bgl*II and *Hind*III. The digestion produced a gene sequence of 147 bp.

The ligation between Cox8a-flag and pGL3-basic-luc was achieved by the ligase reaction and subsequent transformation into One Shot® TOP10 Competent Cells (Figure 25). Correct clones were screened for by colony PCR (Figure 25B).

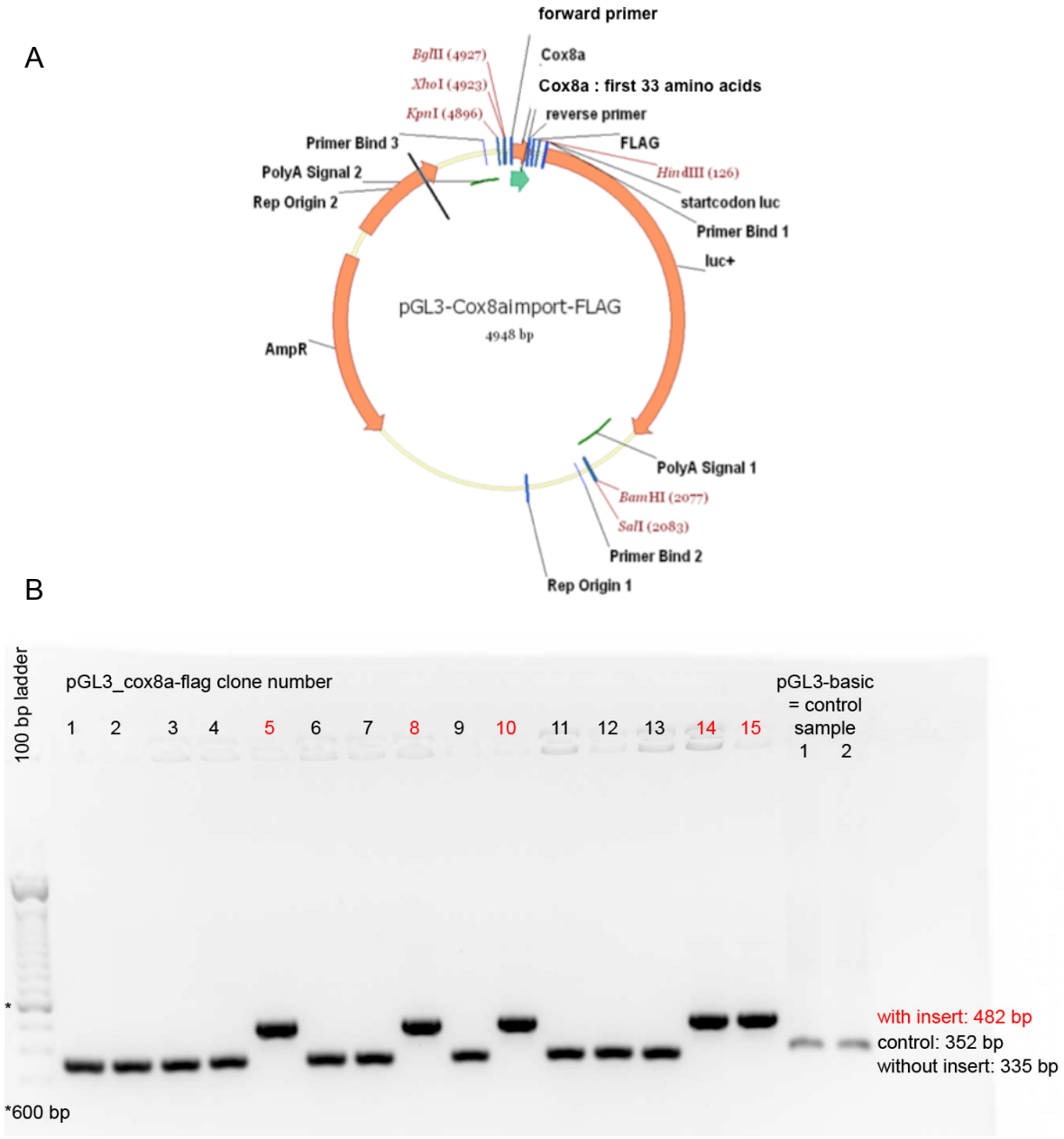

Figure 25: Ligation of pGL3-basic with *cox8a-flag* fragment. (A) Vector map of pGL3_cox8a-flag-luc. (B) Result of colony PCRs after ligation of pGL3-basic and *cox8a-flag* and transformation of *One Shot® TOP10 Competent Cells*. The expected product had a length of 482 bp. A total of 5 clones had this length**.**

7.1.3 The pENTR1A_DS_cox8a-flag-luc entry clone

One Shot® ccdB Survival Cells were transformed with the vector pENTR1A_DS that contains the *ccdB* gene. After DNA preparation, the vector was digested with *BamH*I and *Xho*I (Figure 26) and ligated with the *cox8a-flag-luc* fragment (Figure 27).

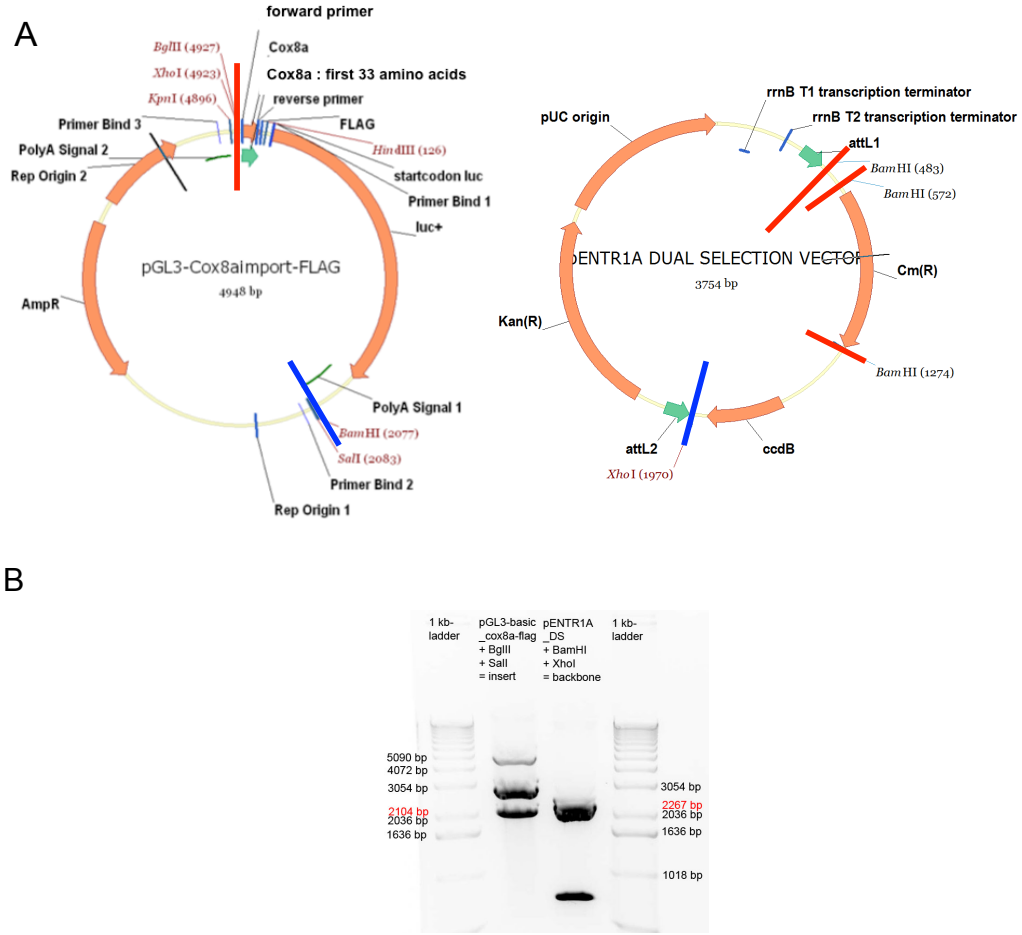

Figure 26: Restriction enzyme digestion of pENTR1A_DS and pGL3-basic_cox8a-flag. (A) Vector maps of both vectors with the inserts. (B) Gel electrophoresis result of the digested vectors pGL3-basic_cox8a-flag and pENTR1A_DS.

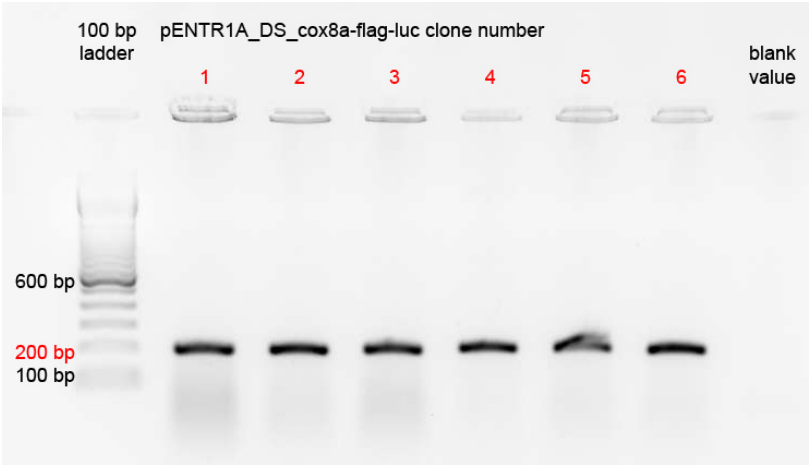

Figure 27: Results of colony PCR on *One Shot*® *TOP10 Competent Cells* transformed with pENTR1A_DS_cox8a-flag-luc.

7.1.4 pROSA26_cox8a-flag-luc

The recombinase reaction was used to finally introduce the gene of interest, *cox8a-flag-luc*, into the destination vector pROSA26-DEST (Figure 28).

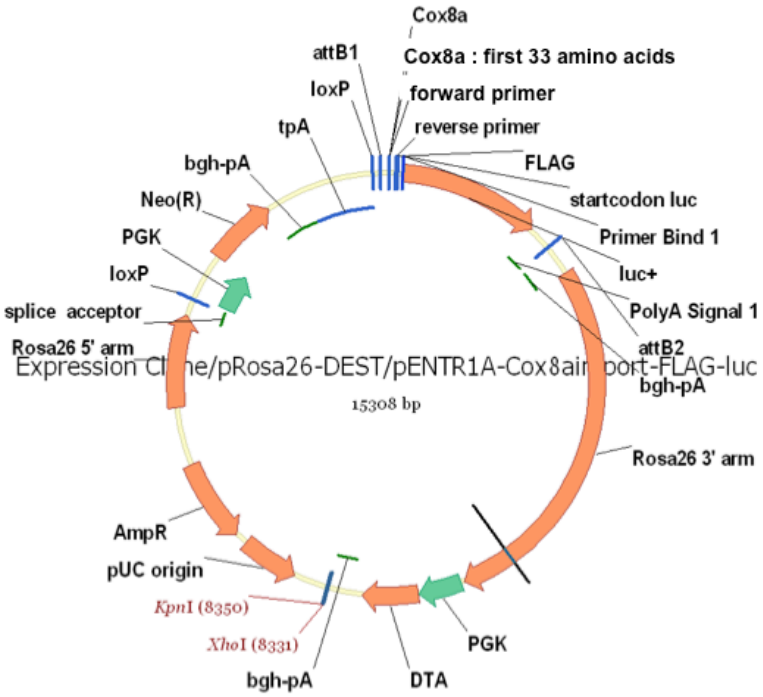

Figure 28: The vector map of pROSA26_cox8a-flag-luc after the recombinase reaction of pROSA26-DEST and pENTR1A_cox8a-flag-luc.

After transformation of *One Shot® TOP10 Competent Cells* and agar plate culture, I performed a colony PCR with two different primer sets (Figure 29). I sequenced both clones to check them on the nucleotide level and I did not find any nucleotide changes. Larger quantities of plasmid were then prepared by midiprep (Qiagen) and controlled by the restriction fragment pattern for *Eco*RI, *Hind*II, and *Sal*I (Figure 29).

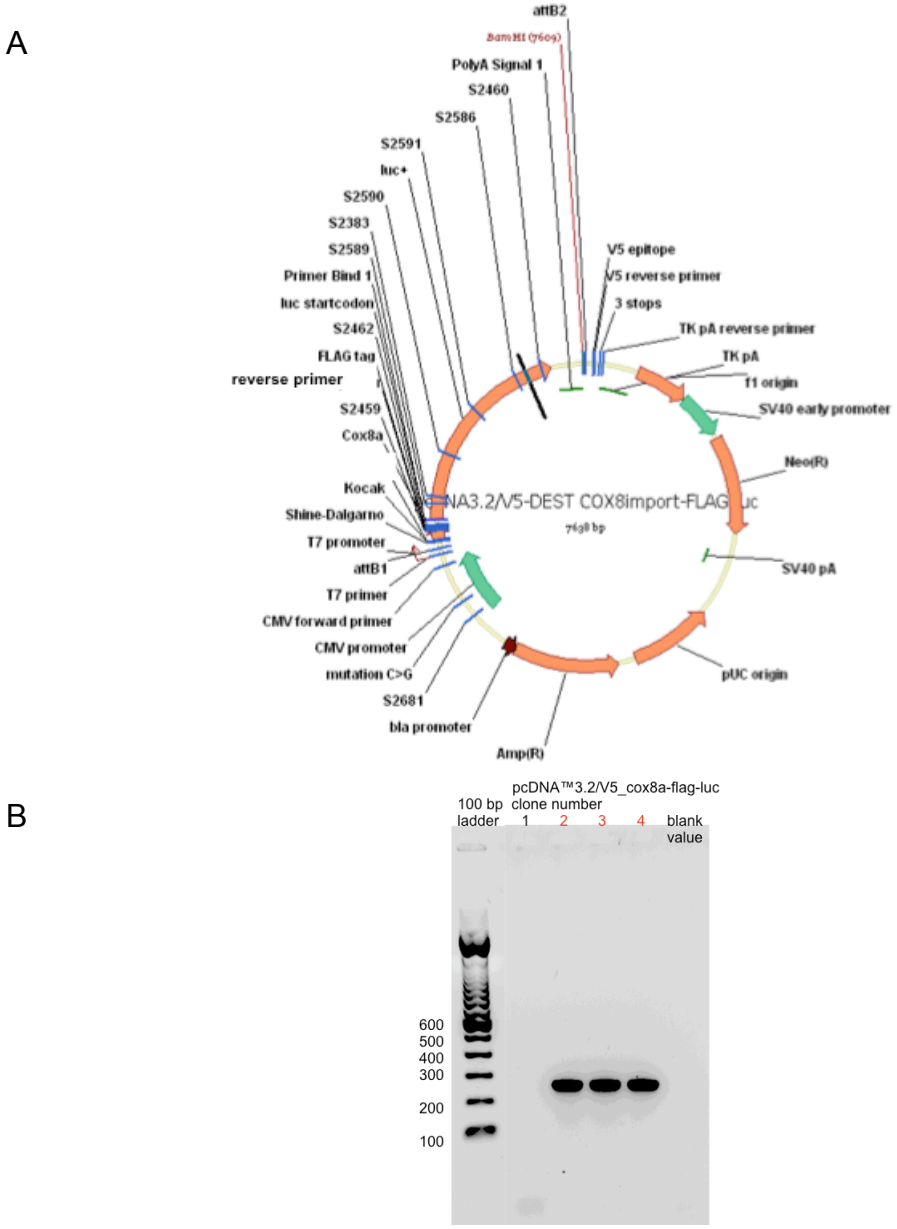

Figure 29: pcDNA3.2/V5_cox8a-flag-luc. (A) Vector map of pcDNA3.2/V5_cox8a-flag-luc. (B) Result of a PCR verifying the *cox8a-flag-luc* insert in the pcDNA™3.2/V5-DEST vector after transformation and overnight culture.

7.2 Correct targeting of the cox8a-luc-FLAG protein to the mitochondria

7.2.1 Detection of the luciferase protein by Western blot

In order to show that the Luciferin protein was indeed expressed in the transfected cells, I performed a Western blot after SDS-PAGE of homogenized with pcDNA3.2/V5_cox8a-flag-luc transfected HEK293 cells. The fusion protein was labeled with an anti-FLAG antibody. Tubulin

was used as loading control. The Western Blot shows a band size of about 70 kDa which was expected.

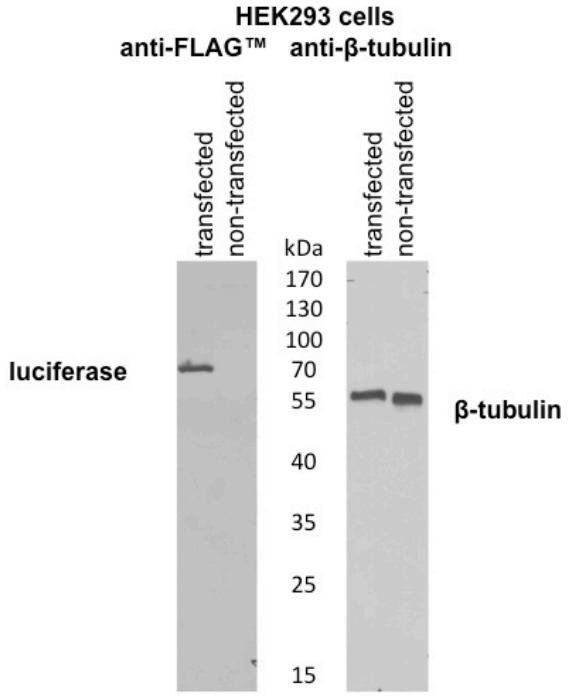

Figure 30: Western blot analysis. Western blot of HEK293 cells transfected with pcDNA3.2/V5_cox8a-flag-luc and untransfected control cells show a ≈70 kDa band only in the transfected cells.

7.3 Cell culture experiments

7.3.1 Immunofluorescence – verification of correct mitochondrial targeting

HEK293 cells and COS1 cells were transfected with pcDNA3.2/V5_cox8a-flag-luc *via* lipofection. I added *MitoTracker® CM-H₂TMRos* which specifically stains active mitochondria of a cell. After fixation, the mitochondria of single cells could be visualized by fluorescence microscopy (Figure 31).

In order to track the protein of interest or the added FLAG™ epitope, I performed an immunocytochemistry assay with an anti-FLAG™ antibody. After binding the secondary antibody, single cells were imaged under excitation light (Figures 31 1B and 2B). Finally, the cells were stained with DAPI in order to mark the nucleus. In contrast to the multiple mitochondria, I saw one spherical nucleus per cell (Figures 31 1C and 2C). In the end, a merged image was taken, unifying the three differently stained items in one picture (Figures 31 1D and 2D).

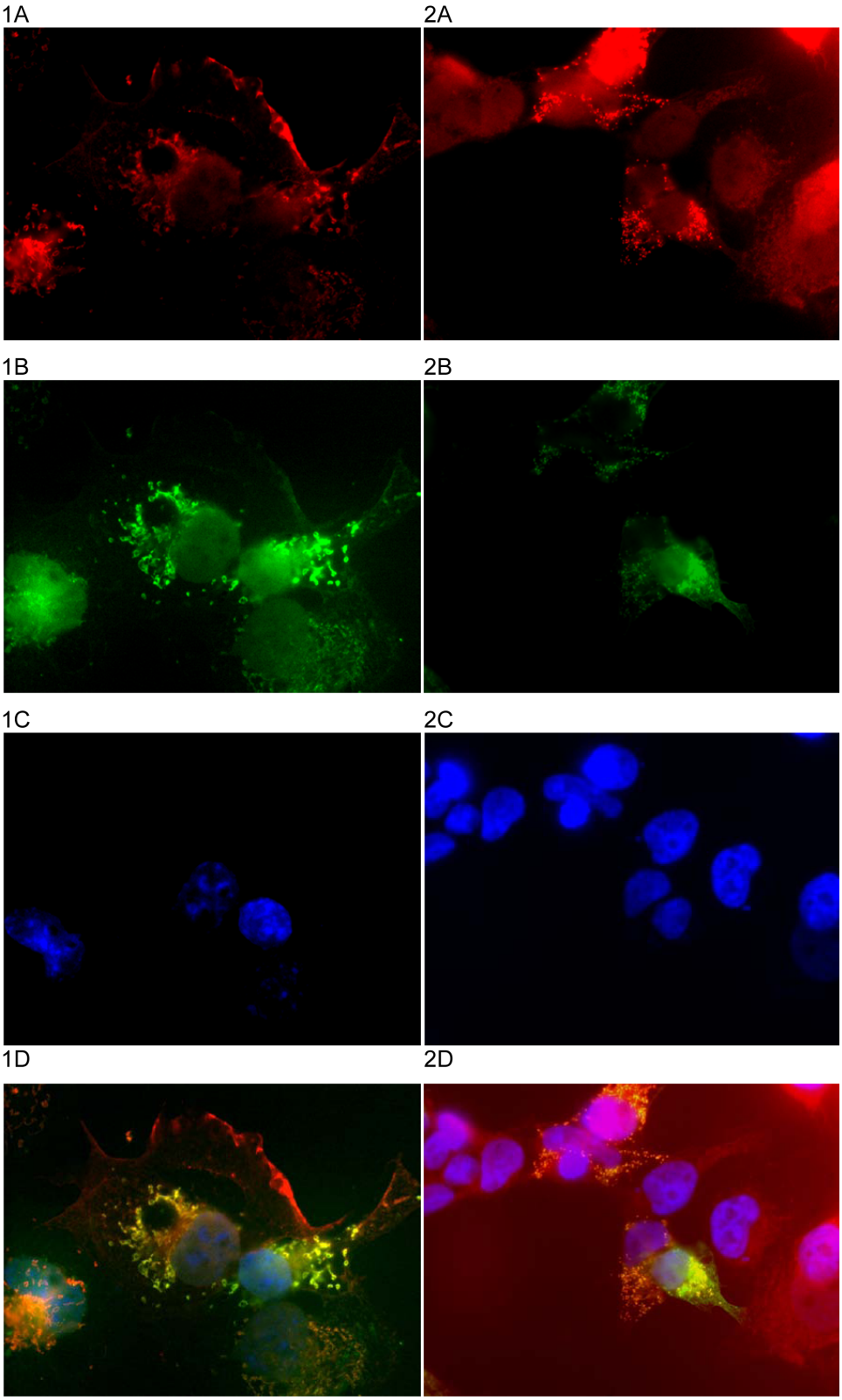

Figure 31: Multicolor fluorescence imaging. (1A-D) HEK293 cells, (2A-D) COS1 cells. Channels: red = anti FLAG antibody, green = *MitoTracker® CM-H_2TMRos*, blue = DAPI, (1D, 2D) overlay. The anti-FLAG and Mito-tracker signals show complete overlay in a characteristic mitochondrial distribution, thus verifying the correct targeting of the Luciferase-FLAG fusion protein at the mitochondria.

7.3.2 Functional testing of luciferase activity

I examined the integrity and function of the translated luciferase protein by means of different luciferin-luciferase assays.

[1] In the first luciferase assay (Figure 32), I compared transfected and untransfected COS1 and HEK293 cells. After adding 100 µl *Bright-Glo™ Luciferase Assay Reagent* (Promega) per well, the luminometer measured equal light emissions in both transfected cell lines and none in the untransfected ones.

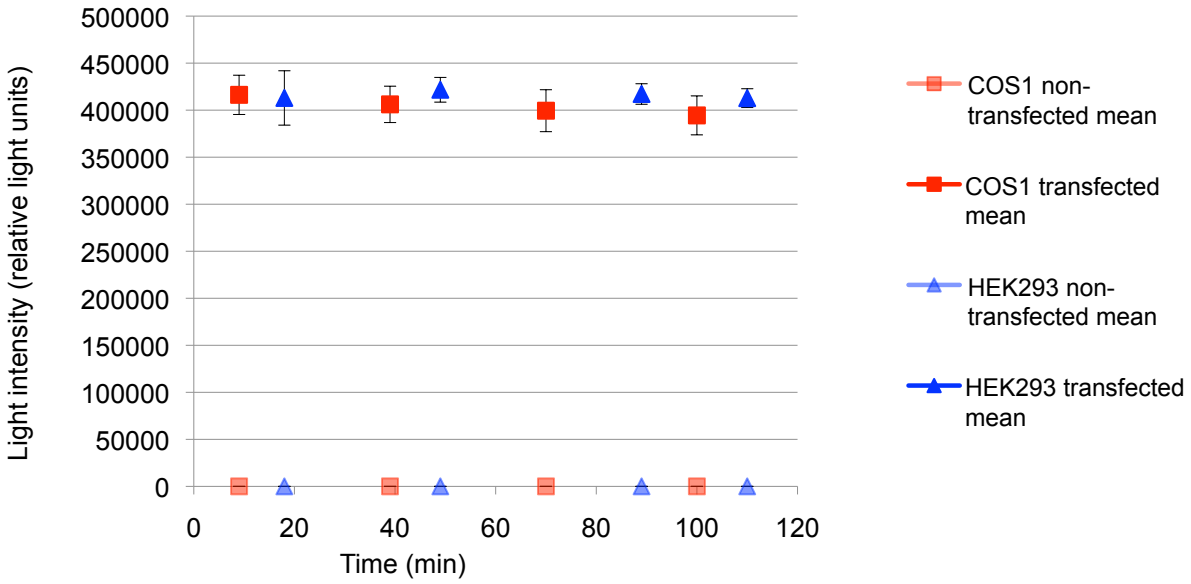

Figure 32: Results of the luciferase assay. pcDNA3.2/V5_cox8a-flag-luc transfected cells were compared to untransfected ones. We see a high light signal in both cell lines. The mean of 3 measurements is shown, the whisker plots show the mean and SEM (n= 3 repetitions).

[2] In the second luciferase assay (Figure 33), I supplemented transfected and non-transfected COS1 cells with 500 µM **ADP** and **increasing amounts of luciferin**. In transfected cells, the light intensity increased, if more luciferin was added, the values of the samples with 2 mM luciferin were about twice as high as those with 0.5 µM luciferin. The graphs of non-transfected cells show a consistent background (zero) line.

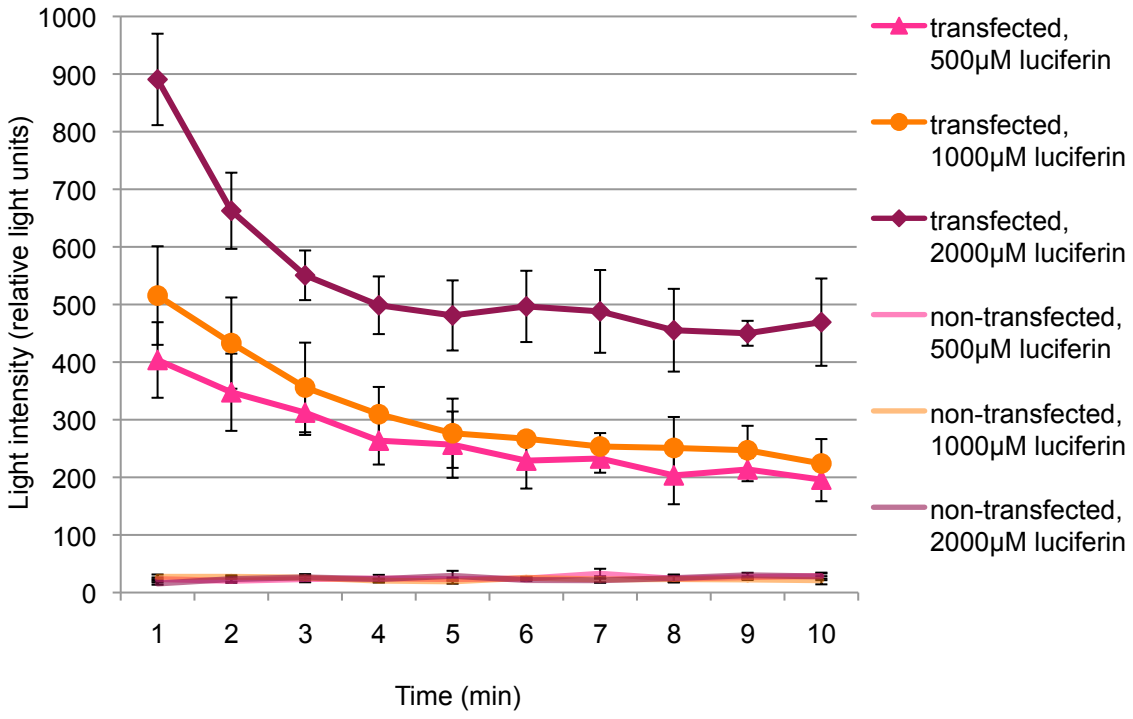

Figure 33: Luciferase assay with transfected and non-transfected cells supplied with 500 µM ADP and increasing amounts of luciferin.

[3] In the third luciferase assay (Figure 34), I grew transfected and non-transfected COS1 cells in the presence of the same amount of luciferin (500 µM), ADP (500 µM) and glutamate/malate (5 mM). The **addition of 500 µM ADP after 20 minutes** to the transfected cells did not result in an increase of light intensity (orange curve). However, the **addition of 500 µM luciferin after 20 minutes** led to an increase of light intensity. This shows that even after 20 min the mitochondria still work on maximum ATP production (which can be stimulated by adding ADP). Hence, the decay in light intensity is only due to the consumption of luciferin.

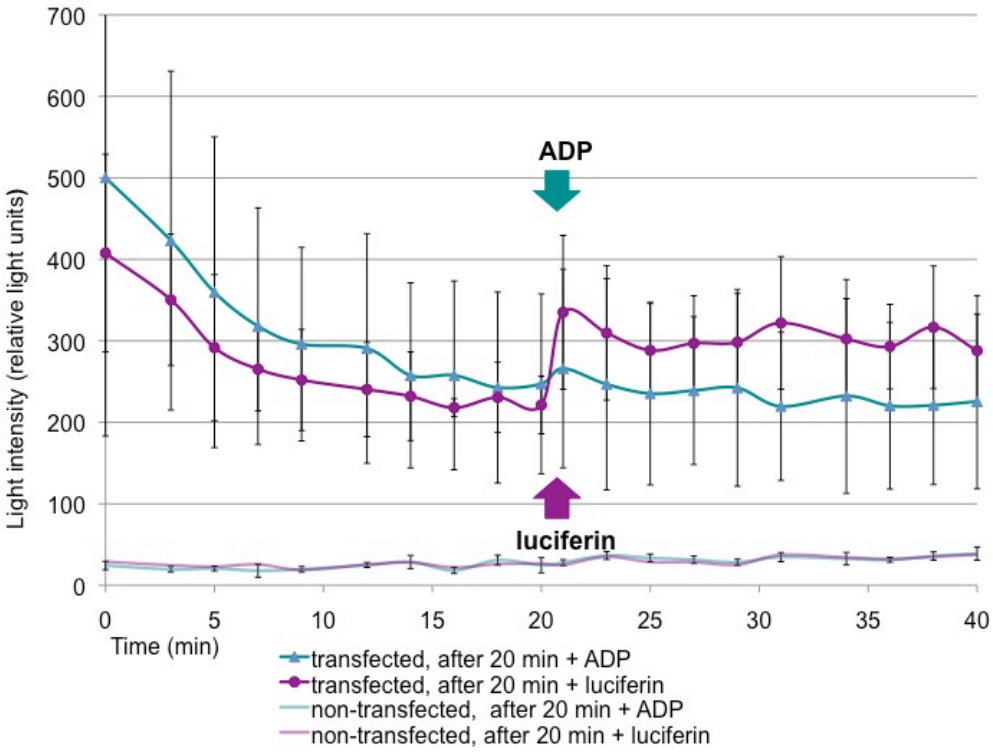

Figure 34: Luciferase assay of transfected COS1 cells after addition of ADP and luciferin. Transfected and non-transfected COS1 cells incubated with 500 µM luciferin, 500 µM ADP, and 5 mM glutamate / malate. After 20 min, 500 µM ADP or 500 µM luciferin was added externally. Data points represent the mean±SEM from 3 repeated measurements.

8 Discussion

The work presented here describes the generation and testing of a molecular tool for the measurement of intra-mitochondrial ATP. As readout, I chose the bioluminescent system of the luciferin-luciferase reaction. The use of the ATP-consuming enzyme luciferase enables us to measure relative ATP levels in the cell *via* quantification of emitted light.[53] The gene of interest, the coding sequence of the luciferase protein, was integrated into a plasmid and altered in such a way that the protein product would be imported into the mitochondria. One vector was created for application in cell culture; another was designed for the generation of a transgenic mouse model.

8.1 Molecular biological methods – vector construction

8.1.1 The ROSA26 locus

Linearized plasmids are well-known and reliable tools to achieve the integration of a gene of interest into an existing genome.[99] Compared to the preparation of viral particles carrying a gene of interest, the preparation of plasmids requires a less sophisticated S1-laboratory setup. In comparison to the infection with viral particles, the transfection and integration rates are much lower if transfected plasmids are used. This drawback, however, can be overcome by the possibility of examining single clones for correct recombination and by co-insertion of a gene (e.g. the neomycin resistance gene) that allows only those cells to grow that have integrated the plasmid. A second consideration should be the locus of integration. Many vectors for the generation of transgenic animals integrate randomly, thereby often destroying the gene they are inserted to. This risk should be minimized. Hence I chose for integration the ROSA26 locus of the mouse that was first discovered and used by Friedrich and Soriano in the course of a gene-trap mutagenesis screening experiment in mouse embryonic stem cells.[100] The ROSA26 locus is a defined section of mouse chromosome 6.[101] It was shown that the insertion of a gene construct into the ROSA26 locus does not result in an altered phenotype.[100] Additionally, the knock-in at ROSA26 locus was shown not to carry the risk of random integration or gene silencing through epigenetic modifications. Another advantage is its continuous and reliable expression in adult mice tissues.[100] Therefore the targeting of gene constructs into the ROSA26 locus represents a reliable method for the creation of transgenic mouse models and it is widely used today. Recently, the analogous human locus could be identified, which probably provides new opportunities for the development of gene therapies.[102]

A highly reliable vector integrating into the ROSA26 locus was first developed by Hastie and his research group in the year 2008.[103] Their work resulted in a vector that is compatible with the *Gateway® recombination system*, integrates into the ROSA26 locus of the mouse and leads to a *Cre*-dependent expression of the gene of interest.

8.1.2 The Gateway• recombination system

Prior to the generation of a murine model, functional assays in cell culture models are mandatory. For this reason, I created a vector for expression in mammalian cell lines. I chose the pcDNA™3.2/V5-DEST vector whose predominant advantage is its compatibility with the *Gateway® recombination system*. The application of pcDNA3.2/V5_cox8a-flag-luc in HEK293 cells resulted in detectable protein expression of an intact enzyme of about 70 kDa. The correct function of the luciferase enzyme was proven by functional assays in COS1 cells.

The *Gateway® recombination system* was proposed by Hohenstein.[103] Hartley and his coworkers reported that the reliability of the facilitated subcloning is an important advantage for daily practice, since it is cost- and time-saving.[104] The recombination is specific since the 7 bp core sequence of each *att* site minimises the cross reactivity, hence the directionality of the insertion is maintained. Therefore, the *Gateway® recombination system* bypasses multiple disadvantages of classic molecular cloning methods using restriction endonucleases. First, the use of restriction enzyme digestion is sometimes limited to very few enzymes because some of them might cleave in the gene of interest. Secondly, the technique of the *Gateway® recombination system* is independent of ligation. Finally, once the plasmid with the insert is established, it can be shuttled into various vectors of the *Gateway®* family for use in different organisms. In contrast to other recombination-depending cloning systems, the *Gateway® recombination system* offers a wide variety of destination vectors.[105]

8.1.3 Targeting of the luciferase to the mitochondria

A protein needs a targeting sequence if its final localization within a cell is not the cytosol. There are different targeting sequences for mitochondrial targeting of a protein in existence.[106] Rizzuto *et al.* investigated the mitochondrial targeting system and found that the amino-terminal 33 amino acids of subunit VIII of cytochrome c oxidase are an efficient targeting sequence.[70,71] The successful positioning of the targeted protein could be verified by immunocytochemistry with a specific antibody directed against the protein of interest (here, the luciferase protein or the FLAG tag). In my work, the colocalization study using a fluorescent *anti-FLAG™* antibody and a

chemical compound that is specifically taken up by the mitochondria (*MitoTracker® CM-H_2TMRos*) verified the correct targeting of the luciferase-FLAG fusion protein.

HEK293 cells are widely used as expression tools and are known for their reliable protein production.[107] In my research work, transfection of HEK293 cells resulted in an acceptable luciferase protein production. However, as HEK293 cells are genetically transmuted by adenovirus type 5 DNA, they might have been altered with regard to mitochondrial function or with regard to other metabolic capabilities.[108] Hence, I performed most of the experiments in parallel with COS1 cells.[109] Transfected COS1 cells as well as transfected HEK293 cells yielded similar results in the luciferase assay, when the same amount of DNA was applied (see Figure 32).

8.2 Cell culture experiments

8.2.1 Immunofluorescence

In order to facilitate the localization of the protein of interest *via* immunofluorescence, I added the recognition sequence of the FLAG™ epitope to the *luc* gene. Due to its shortness and its hydrophilic character, the FLAG™ epitope in most cases does not interact with the attached protein of interest.[92] Hopp and colleagues presented a highly reliable monoclonal antibody that binds to the amino acid sequence and allows tracking or purification of the protein attached. In the meantime, two additional antibodies had been developed.[93] In this work, the anti-FLAG® M2 monoclonal antibody was used whose binding is calcium-independent and that recognizes both *N*-terminal FLAG™ and *C*-terminal FLAG™ fusion proteins.[93]

Visualization of mitochondria is possible by means of mitochondria-specific, cationic dyes, as for example the staining reagent *MitoTracker® CM-H_2TMRos*, that stains living mitochondria and is even preserved after fixation and permeabilization of cells.[96] A disadvantage of *MitoTracker®* stains is their dependence on the mitochondrial membrane potential for mitochondrial import. Hence, ex vivo tissues do not stain and mitochondria that have lost their membrane potential due to a mitochondrial disease would not be seen by the *MitoTracker®* dyes. Moreover, *MitoTracker® CM-TMRos* is known to inhibit complex I of the respiratory chain.[110] This was not a drawback in the context of my work, since the proof of function of the enzyme luciferase was not done in stained cells.

8.2.2 ATP measurement *via* the luciferase assay

I am not aware of any technique for direct measurement of ATP in cells. Therefore ATP has to be determined indirectly. Currently, the most common method is the luciferin-luciferase assay.[42] The coding sequence of the protein luciferase is well-known, it is possible to introduce it *via* recombination into mammalian cells, and the consumption of ATP by the enzyme luciferase does not affect regular processes of the cell.[42] In my experiment, transfection of mammalian cell lines (HEK293 and COS1) with a plasmid containing the luciferase gene sequence was successful. I verified this by means of Western blot, by co-localization analysis and finally by a metabolic assay (luciferase assay).

Time-saving reagents and kits as for example *Bright-Glo™ Luciferase Assay* can be purchased commercially. I was able to show that the light intensity was kept up in cell culture for several minutes before slowly declining over the next hour. The light intensity directly depended on the concentration of luciferin and the decline in the light emission was due to the consumption of luciferin by the reaction. Several factors may influence the light emission: **(1)** pH and ion concentrations (Ca^{2+}, Mg^{2+}), **(2)** the presence of proteolytical enzymes inside the cell (e.g. the proteasome), especially in mammalian cells.[63] Probably, the *Bright-Glo™ Luciferase Assay Reagent* contains biologically inactive analogs of luciferin in order to protect the luciferase protein against proteolytic attack. However, the company does not publish the exact mechanism. **(3)** Finally, the ratio of ATP to luciferin is important.[44]

Beyond that, two more factors may influence the results of luciferase assays. First, the equilibrium of the luciferase reaction can be influenced by downstream reactions. I have shown a correlation between the concentration of luciferin and the light intensity (Figure 33), which has already been shown by Jouaville.[60] However, this proportion is not linear, a fact that in general precludes the absolute measurement of ATP concentrations in the cell but only of relative ATP levels *via* artificial relative light units (RLU). Additionally, the concentration of the luciferase enzyme itself plays an important role.[59] This point I was unable to investigate in my cell-based assay because it would have been difficult to determine the exact luciferin content per cell or per mitochondrion, which would have required a highly sensitive ELISA assay, which was not available. This can be considered as a critical point in the evaluation of the functionality of my vector system. Second, the ATP synthesis by the respiratory chain can be altered by the addition of substrates (glutamate, malate, ADP). I performed different experiments in order to find determinants that influence the light intensity. I was able to show that luciferin is consumed during the reaction which manifests itself as a decline of signal over time. That effect can be reversed by addition of luciferin during the reaction (Figure 34). Interestingly, adding ADP during the

reaction did not enhance the light output. This shows that the mitochondrial respiratory chain, even after 20 minutes, is still maximally stimulated by initial ADP concentration. A further disadvantage of the luciferase assay is its low signal level,[111] which influences the temporal and spatial detection of ATP. The low light intensity does not allow single cell studies under the microscope but only summary assays of several thousand cells in a luminometer. To counteract these disadvantages, other techniques were developed in recent years.

8.2.3 ATP measurement *via* patch clamp technique

Gribble and her coworkers proposed the use of a mutant ATP-sensitive potassium channel as a biosensor to measure ATP concentration directly under the plasma membrane.[112] The measured variable is the variation of the current amplitude through a single potassium channel. The electrophysiological method applied is that of the patch clamp technique.[113] The mutant channel has a truncated subunit and is inhibited by ATP, but not activated by MgADP.[112] However, one has to consider that the concentration of ATP can be within the normal range despite an alteration of the maximum rate of ATP synthesis due to a decrease of the proton electrochemical potential gradient in a quiescent cell.[114] Simultaneous measurement of the changes of the membrane potential could be used for normalization while performing the above mentioned techniques of direct ATP measurement.[115]

8.2.4 ATP measurement *via* fluorescence imaging

A third method that allows both quantification of ATP levels and exact localization of ATP applies fluorescence imaging. One approach is based on fluorescence resonance energy transfer, which is also called **Förster resonance energy transfer** (FRET).[116,117] In the case of subplasmalemmal ATP identification, the first biosensor was constructed with a subunit of an ATP-sensitive potassium channel in order to investigate its conformational changes.[118] In 2009, Imamura *et al.* presented a FRET-based indicator for measuring ATP concentration in different cellular compartments in living cells.[119] The problem of FRET-based biosensors is the time lag of maturation of the two chromophores. When a chromophore is synthesized, further reactions are needed until it is fluorescent. If the two different chromophores have maturation processes of different duration, incomplete sensors alter the result of measurement. In order to bypass this problem, Yaginuma *et al.* proposed a single circularly-permuted fluorescent protein bound to *Bacillus subtilis* F_oF_1-ATP synthase subunit ε.[120] The bonding of ATP induces a change in the intensity of fluorescence. This construct was proven to be able to detect ATP concentrations in single bacterial cells. The measurement was independent of bacterial growth rate and pH.

9 Outlook

The construction of the pcDNA3.2/V5_cox8a-flag-luc vector facilitates the insertion of the luciferase gene into different expression systems due to its compatibility with the *Gateway® recombination system*. The vector was tested in HEK293 and COS1 cells and resulted in high - level gene expression of a working protein of interest. The vector can now be used for measuring mitochondrial ATP production and for the development of drug screening approaches, e.g. for screening drugs approved by the U.S. Food and Drug Administration in patient cells that had been transfected with my plasmid. A direct readout of mitochondrial ATP production via measurement of light would greatly facilitate and accelerate this screening process.

The second plasmid, pROSA26_cox8a-flag-luc, was constructed in order to generate a transgenic, knock-in mouse model that enables *in-vivo* detection of ATP produced in the mitochondria. This mouse model can then be used to study the ATP turnover and mitochondrial ATP production in various organs in healthy animals and in experimental animals with mitochondrial disorders. It would thus be possible to investigate chemical compounds or small molecules in a whole organism that had shown promise in the high-content screening process.

Interestingly, the concept of (only) impaired ATP synthesis as “the” common feature of mitochondrial disorders has recently been questioned. Studies have shown that impairment of a single respiratory chain complex does not automatically results in reduced ATP synthesis.[34,121] The significance of this fact in the context of mitochondrial disorders in humans is not yet clear. The mouse model would be an ideal tool to shed light also on these aspects and biochemical alterations caused by mitochondriopathies.

10 References

1. Schatz G. Jeff's views on science and scientists. Amsterdam, Boston: Elsevier; 2006.
2. De Vos KJ, Sheetz MP. Visualization and quantification of mitochondrial dynamics in living animal cells. Methods Cell Biol 2007;80:627–82.
3. Palade GE. An Electron Microscope Study of the Mitochondrial Structure. J Histochem Cytochem 1953;1(4):188–211.
4. Franke WW, Kartenbeck J. Outer mitochondrial membrane continuous with endoplasmic reticulum. Protoplasma 1971;73(1):35–41.
5. Morré DJ, Merritt WD, Lembi CA. Connections between mitochondria and endoplasmic reticulum in rat liver and onion stem. Protoplasma 1971;73(1):43–9.
6. Wang H-J, Guay G, Pogan L, Sauvé R, Nabi IR. Calcium Regulates the Association between Mitochondria and a Smooth Subdomain of the Endoplasmic Reticulum. J Cell Biol 2000;150(6):1489–98.
7. Bereiter-Hahn J, Jendrach M. Mitochondrial dynamics. Int Rev Cell Mol Biol 2010;284:1–65.
8. Siekevitz P. Powerhouse of the Cell. Sci Am 1957;197(1):131–44.
9. Nicholls DG, Budd SL. Mitochondria and Neuronal Survival. Physiol Rev 2000;80(1):315–60.
10. Mitchell P. Chemiosmotic coupling in oxidative and photosynthetic phosphorylation. Biochim Biophys Acta BBA - Bioenerg 2011;1807(12):1507–38.
11. Potter VR, DuBois KP. Studies on the Mechanism of Hydrogen Transport in Animal Tissues. J Gen Physiol 1943;26(4):391–404.
12. Kaniuga Z, Slater E. Inhibitors around the antimycin-sensitive site. In: Inhibitors: Tools in Cell Research. New York, Heidelberg, Berlin: Springer-Verlag; 1969. p. 282–300.
13. Rieske JS. Inhibitors of respiration at energy-coupling site 2 of the respiratory chain. Pharmacol Ther 1980;11(2):415–50.
14. Thierbach G, Reichenbach H. Myxothiazol, a new inhibitor of the cytochrome b-c1 segment of th respiratory chain. Biochim Biophys Acta 1981;638(2):282–9.
15. von Jagow G, Ljungdahl PO, Graf P, Ohnishi T, Trumpower BL. An inhibitor of mitochondrial respiration which binds to cytochrome b and displaces quinone from the iron-sulfur protein of the cytochrome bc1 complex. J Biol Chem 1984;259(10):6318–26.
16. Anderson S, Bankier AT, Barrell BG, de Bruijn MH, Coulson AR, Drouin J, Eperon IC, Nierlich DP, Roe BA, Sanger F, Schreier PH, Smith AJ, Staden R, Young IG. Sequence and organization of the human mitochondrial genome. Nature 1981;290(5806):457–65.
17. Gray MW. Origin and evolution of organelle genomes. Curr Opin Genet Dev 1993;3(6):884–90.
18. Cann RL, Stoneking M, Wilson AC. Mitochondrial DNA and human evolution. Nature 1987;325(6099):31–6.
19. Brown WM, George M, Wilson AC. Rapid evolution of animal mitochondrial DNA. Proc Natl Acad Sci U S A 1979;76(4):1967–71.
20. Schon EA. Mitochondrial genetics and disease. Trends Biochem Sci 2000;25(11):555–60.
21. Robin ED, Wong R. Mitochondrial DNA molecules and virtual number of mitochondria per cell in mammalian cells. J Cell Physiol 1988;136(3):507–13.
22. Shoubridge EA. Mitochondrial DNA diseases: histological and cellular studies. J Bioenerg Biomembr 1994;26(3):301–10.
23. Giles RE, Blanc H, Cann HM, Wallace DC. Maternal inheritance of human mitochondrial DNA. Proc Natl Acad Sci U S A 1980;77(11):6715–9.
24. Wolff JN, Gemmell NJ. Lost in the zygote: the dilution of paternal mtDNA upon fertilization. Heredity 2008;101(5):429–34.
25. Marchington DR, Scott Brown MSG, Lamb VK, van Golde RJT, Kremer JAM, Tuerlings JHAM, Mariman ECM, Balen AH, Poulton J. No evidence for paternal mtDNA transmission to offspring or extra-embryonic tissues after ICSI. Mol Hum Reprod 2002;8(11):1046–9.
26. Kaneda H, Hayashi J, Takahama S, Taya C, Lindahl KF, Yonekawa H. Elimination of paternal mitochondrial DNA in intraspecific crosses during early mouse embryogenesis. Proc Natl Acad Sci U S A 1995;92(10):4542–6.
27. Schwartz M, Vissing J. Paternal inheritance of mitochondrial DNA. N Engl J Med 2002;347(8):576–80.
28. Jenuth JP, Peterson AC, Fu K, Shoubridge EA. Random genetic drift in the female germline explains the rapid segregation of mammalian mitochondrial DNA. Nat Genet 1996;14(2):146–51.
29. Rossignol R, Faustin B, Rocher C, Malgat M, Mazat J-P, Letellier T. Mitochondrial threshold effects. Biochem J 2003;370(Pt 3):751–62.
30. Skladal D, Halliday J, Thorburn DR. Minimum birth prevalence of mitochondrial respiratory

chain disorders in children. Brain J Neurol 2003;126(Pt 8):1905–12.

31. Arpa J, Cruz-Martínez A, Campos Y, Gutiérrez-Molina M, García-Rio F, Pérez-Conde C, Martín MA, Rubio JC, Del Hoyo P, Arpa-Fernández A, Arenas J. Prevalence and progression of mitochondrial diseases: a study of 50 patients. Muscle Nerve 2003;28(6):690–5.
32. Schaefer AM, Taylor RW, Turnbull DM, Chinnery PF. The epidemiology of mitochondrial disorders--past, present and future. Biochim Biophys Acta 2004;1659(2–3):115–20.
33. AWMF. Diagnostik und Therapieansätze bei Mitochondriopathien im Kindes- und Jugendalter. 2011;
34. Bird MJ, Thorburn DR, Frazier AE. Modelling biochemical features of mitochondrial neuropathology. Biochim Biophys Acta 2014;1840(4):1380–92.
35. Zeviani M, Tiranti V, Piantadosi C. Mitochondrial disorders. Medicine (Baltimore) 1998;77(1):59–72.
36. Rubio-Gozalbo ME, Dijkman KP, van den Heuvel LP, Sengers RC, Wendel U, Smeitink JA. Clinical differences in patients with mitochondriocytopathies due to nuclear versus mitochondrial DNA mutations. Hum Mutat 2000;15(6):522–32.
37. DiMauro S. Mitochondrial encephalomyopathies: what next? J Inherit Metab Dis 1996;19(4):489–503.
38. DiMauro S, Schon EA. Mitochondrial respiratory-chain diseases. N Engl J Med 2003;348(26):2656–68.
39. Carrozzo R, Tessa A, Vázquez-Memije ME, Piemonte F, Patrono C, Malandrini A, Dionisi-Vici C, Vilarinho L, Villanova M, Schägger H, Federico A, Bertini E, Santorelli FM. The T9176G mtDNA mutation severely affects ATP production and results in Leigh syndrome. Neurology 2001;56(5):687–90.
40. Visch H-J, Rutter GA, Koopman WJH, Koenderink JB, Verkaart S, de Groot T, Varadi A, Mitchell KJ, van den Heuvel LP, Smeitink JAM, Willems PHGM. Inhibition of mitochondrial Na+-Ca2+ exchange restores agonist-induced ATP production and Ca2+ handling in human complex I deficiency. J Biol Chem 2004;279(39):40328–36.
41. Alberts B. Energy conversion: MItochondria and Chloroplasts. In: Molecular biology of the cell. New York: Garland science; 2002.
42. Bell CJ, Manfredi G, Griffiths EJ, Rutter GA. Luciferase expression for ATP imaging: application to cardiac myocytes. Methods Cell Biol 2007;80:341–52.
43. Brand MD, Nicholls DG. Assessing mitochondrial dysfunction in cells. Biochem J 2011;435(2):297–312.
44. Manfredi G, Yang L, Gajewski CD, Mattiazzi M. Measurements of ATP in mammalian cells. Methods San Diego Calif 2002;26(4):317–26.
45. Clark LC, Wolf R, Granger D, Taylor Z. Continuous recording of blood oxygen tensions by polarography. J Appl Physiol 1953;6(3):189–93.
46. Villani G, Attardi G. In vivo measurements of respiration control by cytochrome c oxidase and in situ analysis of oxidative phosphorylation. Methods Cell Biol 2001;65:119–31.
47. Chance B, Williams GR. Respiratory enzymes in oxidative phosphorylation. I. Kinetics of oxygen utilization. J Biol Chem 1955;217(1):383–93.
48. MitoPedia: Respiratory states - Bioblast [Internet]. [cited 2016 Apr 18];Available from: http://www.bioblast.at/index.php/MitoPedia:_Respiratory_states
49. Greer LF, Szalay AA. Imaging of light emission from the expression of luciferases in living cells and organisms: a review. Lumin J Biol Chem Lumin 2002;17(1):43–74.
50. Rowe L, Dikici E, Daunert S. Engineering bioluminescent proteins: expanding their analytical potential. Anal Chem 2009;81(21):8662–8.
51. Harvey E N. Bioluminescence. New York: Academic Press; 1952.
52. Marques SM, Esteves da Silva JCG. Firefly bioluminescence: a mechanistic approach of luciferase catalyzed reactions. IUBMB Life 2009;61(1):6–17.
53. McELROY WD. Properties of the reaction utilizing adenosinetriphosphate for bioluminescence. J Biol Chem 1951;191(2):547–57.
54. Seliger HH, McELROY WD. Spectral emission and quantum yield of firefly bioluminescence. Arch Biochem Biophys 1960;88:136–41.
55. Demas. The Measurement of Photoluminescence Quantum Yields. 1971;75:991–1024.
56. Seliger HH, McElroy WD. The Colors of Firefly Bioluminescence: Enzyme Configuration and Species Specificity. Proc Natl Acad Sci U S A 1964;52(1):75–81.
57. de Wet JR, Wood KV, Helinski DR, DeLuca M. Cloning of firefly luciferase cDNA and the expression of active luciferase in Escherichia coli. Proc Natl Acad Sci U S A 1985;82(23):7870–3.
58. de Wet JR, Wood KV, DeLuca M, Helinski DR, Subramani S. Firefly luciferase gene: structure and expression in mammalian cells. Mol Cell Biol 1987;7(2):725–37.
59. Neufeld HA, Towner RD, Pace J. A rapid method for determining ATP by the firefly lucife-

rin-luciferase system. Experientia 1975;31(3):391–2.

60. Jouaville LS, Pinton P, Bastianutto C, Rutter GA, Rizzuto R. Regulation of mitochondrial ATP synthesis by calcium: evidence for a long-term metabolic priming. Proc Natl Acad Sci U S A 1999;96(24):13807–12.
61. White EH, McCapra F, Field GF. The Structure and Synthesis of Firefly Luciferin. 1963;85.
62. Seliger HH, McELROY WD, White EH, Field GF. Stereo-specificity and firefly bioluminescence, a comparison of natural and synthetic luciferins. Proc Natl Acad Sci U S A 1961;47:1129–34.
63. Bronstein I, Fortin J, Stanley PE, Stewart GS, Kricka LJ. Chemiluminescent and bioluminescent reporter gene assays. Anal Biochem 1994;219(2):169–81.
64. Airth RL, Rhodes WC, McELROY WD. The function of coenzyme A in luminescence. Biochim Biophys Acta 1958;27(3):519–32.
65. McElroy WD. The Energy Source for Bioluminescence in an Isolated System. Proc Natl Acad Sci U S A 1947;33(11):342–5.
66. Viviani VR. The origin, diversity, and structure function relationships of insect luciferases. Cell Mol Life Sci CMLS 2002;59(11):1833–50.
67. de Wet JR, Wood KV, Helinski DR, DeLuca M. Cloning firefly luciferase. Methods Enzymol 1986;133:3–14.
68. Rutter GA, Kennedy HJ, Wood CD, White MR, Tavaré JM. Real-time imaging of gene expression in single living cells. Chem Biol 1998;5(11):R285-290.
69. Kennedy HJ, Pouli AE, Ainscow EK, Jouaville LS, Rizzuto R, Rutter GA. Glucose generates sub-plasma membrane ATP microdomains in single islet beta-cells. Potential role for strategically located mitochondria. J Biol Chem 1999;274(19):13281–91.
70. Rizzuto R, Nakase H, Darras B, Francke U, Fabrizi GM, Mengel T, Walsh F, Kadenbach B, DiMauro S, Schon EA. A gene specifying subunit VIII of human cytochrome c oxidase is localized to chromosome 11 and is expressed in both muscle and non-muscle tissues. J Biol Chem 1989;264(18):10595–600.
71. Rizzuto R, Brini M, Bastianutto C, Marsault R, Pozzan T. Photoprotein-mediated measurement of calcium ion concentration in mitochondria of living cells. Methods Enzymol 1995;260:417–28.
72. Rozen S, Skaletsky H. Primer3 on the WWW for general users and for biologist programmers. Methods Mol Biol Clifton NJ 2000;132:365–86.
73. Mullis KB, Faloona FA. Specific synthesis of DNA in vitro via a polymerase-catalyzed chain reaction. Methods Enzymol 1987;155:335–50.
74. Saiki RK, Scharf S, Faloona F, Mullis KB, Horn GT, Erlich HA, Arnheim N. Enzymatic amplification of beta-globin genomic sequences and restriction site analysis for diagnosis of sickle cell anemia. Science 1985;230(4732):1350–4.
75. Williams RK, Smith. BSA and Restriction Enzyme Digestion. Promega Notes Mag 1996;59.
76. Roberts RJ, Belfort M, Bestor T, Bhagwat AS, Bickle TA, Bitinaite J, Blumenthal RM, Degtyarev SK, Dryden DTF, Dybvig K, Firman K, Gromova ES, Gumport RI, Halford SE, Hattman S, Heitman J, Hornby DP, Janulaitis A, Jeltsch A, Josephsen J, Kiss A, Klaenhammer TR, Kobayashi I, Kong H, Krüger DH, Lacks S, Marinus MG, Miyahara M, Morgan RD, Murray NE, Nagaraja V, Piekarowicz A, Pingoud A, Raleigh E, Rao DN, Reich N, Repin VE, Selker EU, Shaw P, Stein DC, Stoddard BL, Szybalski W, Trautner TA, Van Etten JL, Vitor JMB, Wilson GG, Xu S. A nomenclature for restriction enzymes, DNA methyltransferases, homing endonucleases and their genes. Nucleic Acids Res 2003;31(7):1805–12.
77. Gellert M. Formation of covalent circles of lambda DNA by E. coli extracts. Proc Natl Acad Sci U S A 1967;57(1):148–55.
78. Weiss B, Richardson CC. Enzymatic breakage and joining of deoxyribonucleic acid, I. Repair of single-strand breaks in DNA by an enzyme system from Escherichia coli infected with T4 bacteriophage. Proc Natl Acad Sci U S A 1967;57(4):1021–8.
79. Olivera BM, Lehman IR. Linkage of polynucleotides through phosphodiester bonds by an enzyme from Escherichia coli. Proc Natl Acad Sci U S A 1967;57(5):1426–33.
80. Gefter ML, Becker A, Hurwitz J. The enzymatic repair of DNA. I. Formation of circular lambda-DNA. Proc Natl Acad Sci U S A 1967;58(1):240–7.
81. Cozzarelli NR, Melechen NE, Jovin TM, Kornberg A. Polynucleotide cellulose as a substrate for a polynucleotide ligase induced by phage T4. Biochem Biophys Res Commun 1967;28(4):578–86.
82. Sanger F, Nicklen S, Coulson AR. DNA sequencing with chain-terminating inhibitors. Proc Natl Acad Sci U S A 1977;74(12):5463–7.
83. Smith LM, Sanders JZ, Kaiser RJ, Hughes P, Dodd C, Connell CR, Heiner C, Kent SBH, Hood LE. Fluorescence detection in automated DNA sequence analysis. Nature 1986;321(6071):674–9.

84. Jorgenson JW, Lukacs KD. Free-zone electrophoresis in glass capillaries. Clin Chem 1981;27(9):1551–3.
85. Jaffé A, Ogura T, Hiraga S. Effects of the ccd function of the F plasmid on bacterial growth. J Bacteriol 1985;163(3):841–9.
86. Bahassi EM, O'Dea MH, Allali N, Messens J, Gellert M, Couturier M. Interactions of CcdB with DNA gyrase. Inactivation of Gyra, poisoning of the gyrase-DNA complex, and the antidote action of CcdA. J Biol Chem 1999;274(16):10936–44.
87. Landy A. Dynamic, structural, and regulatory aspects of lambda site-specific recombination. Annu Rev Biochem 1989;58:913–49.
88. Cohen SN, Chang AC, Hsu L. Nonchromosomal antibiotic resistance in bacteria: genetic transformation of Escherichia coli by R-factor DNA. Proc Natl Acad Sci U S A 1972;69(8):2110–4.
89. Birnboim HC, Doly J. A rapid alkaline extraction procedure for screening recombinant plasmid DNA. Nucleic Acids Res 1979;7(6):1513–23.
90. Shine J, Dalgarno L. The 3'-terminal sequence of Escherichia coli 16S ribosomal RNA: complementarity to nonsense triplets and ribosome binding sites. Proc Natl Acad Sci U S A 1974;71(4):1342–6.
91. Kozak M. An analysis of 5'-noncoding sequences from 699 vertebrate messenger RNAs. Nucleic Acids Res 1987;15(20):8125–48.
92. Hopp TP, Prickett KS, Price VL, Libby RT, March CJ, Cerretti DP, Urdal DL, Conlon PJ. A Short Polypeptide Marker Sequence Useful for Recombinant Protein Identification and Purification. Nat Biotechnol 1988;6.
93. Einhauer A, Jungbauer A. The FLAG peptide, a versatile fusion tag for the purification of recombinant proteins. J Biochem Biophys Methods 2001;49(1–3):455–65.
94. Wolf DE. Fundamentals of fluorescence and fluorescence microscopy. Methods Cell Biol 2013;114:69–97.
95. Lin MS, Comings DE, Alfi OS. Optical Studies of the interaction of 4'-6'-diamidino-2-phenylindole with DNA and metaphase chromosomes. Chromosoma 1977;60(1):15–25.
96. Poot M, Zhang YZ, Krämer JA, Wells KS, Jones LJ, Hanzel DK, Lugade AG, Singer VL, Haugland RP. Analysis of mitochondrial morphology and function with novel fixable fluorescent stains. J Histochem Cytochem Off J Histochem Soc 1996;44(12):1363–72.
97. Bradford MM. A rapid and sensitive method for the quantitation of microgram quantities of protein utilizing the principle of protein-dye binding. Anal Biochem 1976;72:248–54.
98. Greer S, Honeywell R, Geletu M, Arulanandam R, Raptis L. Housekeeping genes; expression levels may change with density of cultured cells. J Immunol Methods 2010;355(1–2):76–9.
99. Alberts BJ, Lewis J. Isolating, Cloning, and Sequencing DNA. In: Molecular biology of the cell. New York: Garland Science; 2002.
100. Friedrich G, Soriano P. Promoter traps in embryonic stem cells: a genetic screen to identify and mutate developmental genes in mice. Genes Dev 1991;5(9):1513–23.
101. Zambrowicz BP, Imamoto A, Fiering S, Herzenberg LA, Kerr WG, Soriano P. Disruption of overlapping transcripts in the ROSA beta geo 26 gene trap strain leads to widespread expression of beta-galactosidase in mouse embryos and hematopoietic cells. Proc Natl Acad Sci U S A 1997;94(8):3789–94.
102. Irion S, Luche H, Gadue P, Fehling HJ, Kennedy M, Keller G. Identification and targeting of the ROSA26 locus in human embryonic stem cells. Nat Biotechnol 2007;25(12):1477–82.
103. Hohenstein P, Slight J, Ozdemir DD, Burn SF, Berry R, Hastie ND. High-efficiency Rosa26 knock-in vector construction for Cre-regulated overexpression and RNAi. PathoGenetics 2008;1(1):3.
104. Hartley JL, Temple GF, Brasch MA. DNA cloning using in vitro site-specific recombination. Genome Res 2000;10(11):1788–95.
105. Celie PH, Parret AH, Perrakis A. Recombinant cloning strategies for protein expression. Curr Opin Struct Biol 2016;38:145–54.
106. Glover LA, Lindsay JG. Targeting proteins to mitochondria: a current overview. Biochem J 1992;284 (Pt 3):609–20.
107. Thomas P, Smart TG. HEK293 cell line: a vehicle for the expression of recombinant proteins. J Pharmacol Toxicol Methods 2005;51(3):187–200.
108. Graham FL, Smiley J, Russell WC, Nairn R. Characteristics of a human cell line transformed by DNA from human adenovirus type 5. J Gen Virol 1977;36(1):59–74.
109. Gluzman Y. SV40-transformed simian cells support the replication of early SV40 mutants. Cell 1981;23(1):175–82.
110. Scorrano L, Petronilli V, Colonna R, Di Lisa F, Bernardi P. Chloromethyltetramethylrosamine (Mitotracker Orange) induces the mitochondrial permeability transition and inhibits respiratory complex I. Implications for the mechanism of cytochrome c release. J Biol Chem 1999;274(35):24657–63.
111. Berg J, Hung YP, Yellen G. A genetically encoded fluorescent reporter of ATP:ADP ratio. Nat Methods 2009;6(2):161–6.

112. Gribble FM, Loussouarn G, Tucker SJ, Zhao C, Nichols CG, Ashcroft FM. A novel method for measurement of submembrane ATP concentration. J Biol Chem 2000;275(39):30046–9.

113. Sakmann B, Neher E. Patch clamp techniques for studying ionic channels in excitable membranes. Annu Rev Physiol 1984;46:455–72.

114. James AM, Sheard PW, Wei YH, Murphy MP. Decreased ATP synthesis is phenotypically expressed during increased energy demand in fibroblasts containing mitochondrial tRNA mutations. Eur J Biochem FEBS 1999;259(1–2):462–9.

115. Tarasov AI, Rutter GA. Use of genetically encoded sensors to monitor cytosolic ATP/ADP ratio in living cells. Methods Enzymol 2014;542:289–311.

116. Förster T. Zwischenmolekulare Energiewanderung und Fluoreszenz. Ann Phys 1948;437:55–75.

117. Liemburg-Apers DC, Imamura H, Forkink M, Nooteboom M, Swarts HG, Brock R, Smeitink JAM, Willems PHGM, Koopman WJH. Quantitative glucose and ATP sensing in mammalian cells. Pharm Res 2011;28(11):2745–57.

118. Tsuboi T, Lippiat JD, Ashcroft FM, Rutter GA. ATP-dependent interaction of the cytosolic domains of the inwardly rectifying K+ channel Kir6.2 revealed by fluorescence resonance energy transfer. Proc Natl Acad Sci U S A 2004;101(1):76–81.

119. Imamura H, Nhat KPH, Togawa H, Saito K, Iino R, Kato-Yamada Y, Nagai T, Noji H. Visualization of ATP levels inside single living cells with fluorescence resonance energy transfer-based genetically encoded indicators. Proc Natl Acad Sci U S A 2009;106(37):15651–6.

120. Yaginuma H, Kawai S, Tabata KV, Tomiyama K, Kakizuka A, Komatsuzaki T, Noji H, Imamura H. Diversity in ATP concentrations in a single bacterial cell population revealed by quantitative single-cell imaging. Sci Rep 2014;4:6522.

121. Alam MT, Manjeri GR, Rodenburg RJ, Smeitink JAM, Notebaart RA, Huynen M, Willems PHGM, Koopman WJH. Skeletal muscle mitochondria of NDUFS4-/- mice display normal maximal pyruvate oxidation and ATP production. Biochim Biophys Acta 2015;1847(6–7):526–33.

11 Appendix

11.1 Affirmation in lieu of an oath

„Ich, Friederike Wilbert, versichere an Eides statt durch meine eigenhändige Unterschrift, dass ich die vorgelegte Dissertation mit dem Thema: „***Development of a transgenic animal model for measurement of intra-cellular ATP***“ selbständig und ohne nicht offengelegte Hilfe Dritter verfasst und keine anderen als die angegebenen Quellen und Hilfsmittel genutzt habe.
Alle Stellen, die wörtlich oder dem Sinne nach auf Publikationen oder Vorträgen anderer Autoren beruhen, sind als solche in korrekter Zitierung (siehe „Uniform Requirements for Manuscripts (URM)“ des ICMJE -*www.**icmje**.org*) kenntlich gemacht. Die Abschnitte zu Methodik (insbesondere praktische Arbeiten, Laborbestimmungen, statistische Aufarbeitung) und Resultate (insbesondere Abbildungen, Graphiken und Tabellen) entsprechen den URM (s.o) und werden von mir verantwortet.

Die Bedeutung dieser eidesstattlichen Versicherung und die strafrechtlichen Folgen einer unwahren eidesstattlichen Versicherung (§156,161 des Strafgesetzbuches) sind mir bekannt und bewusst.

Datum Unterschrift

11.2 Curriculum vitae

"Mein Lebenslauf wird aus datenschutzrechtlichen Gründen in der elektronischen Version meiner Arbeit nicht veröffentlicht."

11.3 Publication

Brinckmann A, Weiss C, **Wilbert F**, von Moers A, Zwirner A, Stoltenburg-Didinger G, Wilichowski E, Schuelke M: Regionalized pathology correlates with augmentation of mtDNA copy numbers in a patient with myoclonic epilepsy with ragged-red fibers (MERRF-syndrome). PLoS One. 2010 Oct 20;5(10):e13513. doi: 10.1371/journal.pone.0013513.

11.4 Acknowledgment

I would like to express my gratitude to all those, who contributed to the realization and completion of the dissertation in multiple ways.

Special thanks go to Professor Markus Schülke-Gerstenfeld for giving me the chance to perform an experimental doctoral thesis, the professional supervision, the continuous commitment and the excellent support during the last years.

Sincere thanks are given to all of the former and present members of the work group for the good teamwork, the comfortable working atmosphere and the tips and tricks for the daily laboratory work. I thank especially Susanne Lützkendorf for her straightforward help, the reliable maintenance of the cell culture and the performance of the luciferase assays. In the same manner I would like to thank Barbara Lucke for her technical support and the realization of the sequencing. I deeply appreciate the ongoing and motivating support of Dr. Anne van Riesen.

Finally, I sincerely thank my family for their generous and constant support. I thank all my friends for their sympathetic and motivating companionship.